LHCb-PUB-2016-005
March 17, 2016

Calibration samples for particle identification at LHCb in Run 2

L. Anderlini[1], V. V. Gligorov[2], O. Lupton[3], B. Sciascia[4]

[1]*Sezione INFN di Firenze, Firenze, Italy*
[2]*LPNHE, Université Pierre et Marie Curie, Université Paris Diderot, CNRS/IN2P3, Paris, France*
[3]*Department of Physics, University of Oxford, Oxford, United Kingdom*
[4]*Laboratori Nazionali dell'INFN di Frascati, Frascati, Italy*

Abstract

The strategy for data-driven determination of particle identification performance at LHCb has changed significantly from Run 1 to Run 2 of the LHC. This note outlines these changes, explains the rationale behind them and summarises the new system and configuration.

Contents

List of Figures

List of Tables

1 Introduction

The majority of physics analyses using data from the LHCb detector [1] rely on Particle Identification (PID) variables to separate charged tracks of different species; pions, kaons, protons, electrons and muons. In Run 2 of the LHC, which began in 2015, information from the Ring Imaging Cherenkov (RICH) detectors and calorimeter (CALO) systems is included in the full event reconstruction performed in the second level software trigger, HLT2 [2]. Information from the MUON system was already available in the hardware and software triggers in Run 1. This additional information, coupled with the novel real-time detector alignment and calibration introduced for Run 2 [3], allows selections in HLT2 to take advantage of offline-quality PID discriminating variables. These variables are used extensively in HLT2 selections to increase signal purity, reduce the processing time required to reconstruct high-multiplicity signal decays, and allow selections to reduce biases on quantities of physical interest, such as decay time.

This extensive use of PID variables as selection criteria in LHCb analyses – in both LHC runs – has necessitated the development of data-driven methods for measuring the performance of such requirements. The alternative, measuring performance from simulated samples, is undesirable as the PID variables are known to be poorly reproduced, and for some purposes it is difficult to accumulate a sufficiently large sample of simulated events. The data-driven methods are based on calibration samples; pure samples of charged tracks of different species that have been selected without the use of PID information from the RICH, CALO or MUON systems. In addition to being used in physics analyses, these samples can be used to monitor temporal variations in performance, and to study future improvements in reconstruction algorithms.

In Run 2, the requirements for the calibration samples have become more stringent. A more complete discussion is given in Ref. [4], but in brief the widespread use of PID variables in HLT2, which may have small differences with respect to the same variables calculated offline, means that the calibration samples must contain both HLT2-calculated and offline-calculated PID variables on a track-by-track basis. These differences are small, and confined to variables based on CALO information, in data recorded in 2015, but future improvements in the offline algorithms could enhance the differences in future re-analysis of these data. In order to satisfy the various requirements, the strategy for Run 2 is to select the calibration samples directly in HLT2 and send them through a dedicated data processing stream.

This note describes the HLT2 selections implemented for Run 2, covering three periods of pp data-taking: the early measurements (EM) period during the 50 ns bunch-spacing LHC intensity ramp, the 25 ns bunch-spacing data-taking that followed this, and a proposed configuration for 2016 running. The sample yields and purities found in the 25 ns bunch-spacing sample recorded in 2015 are also summarised.

2 Outline of selection strategy

The HLT2 selections are designed to select pure samples of the five most common charged, long-lived particle species produced in LHCb: kaons, pions, protons, electrons and muons. Generally low-multiplicity decay modes with large branching fractions are chosen; an overview of the utilised modes is given in Table 1. Some decays, such as the $D^{*+} \to D^0\pi^+$, $D^0 \to K^-\pi^+$ decay[1] chain that is the primary source of kaon and pion calibration tracks, are selected without the use of PID variables. Other modes, such as the $J/\psi \to \mu^+\mu^-$ decays used to obtain muon calibration samples, rely on a tag-and-probe method where PID requirements are made on one of the two muons. In all cases the selections are designed to ensure the hardware (L0) and first level software (HLT1) triggers do not bias the distributions of PID variables in the calibration samples. The L0 trigger uses information from the CALO and MUON systems to reduce the rate at which the full detector is read out to around 1 MHz. Inclusive selections based on one or two tracks and information from the CALO and MUON systems are performed by HLT1.

The calibration samples are selected directly in HLT2 in Run 2, in contrast to Run 1 when the samples were selected offline. One reason for this, discussed in the introduction, is that the use of PID variables in the Run 2 HLT2 is much more widespread than during Run 1. Another reason is that the selection efficiency for some calibration modes can be greatly improved, for instance $\Lambda^0 \to p\pi^-$ decays where the proton has particularly high p_T. This is illustrated in Sect. 4. HLT2 records events in several streams:

- **Full** This is similar to Run 1, minimal information is persisted from HLT2 and analysis relies on the offline reconstruction.
- **Turbo** Sufficient information is persisted from HLT2 that no offline reconstruction is required before physics analysis [5]. In principle the raw event information is discarded to save storage space, although in practice this information was retained during 2015 data-taking.
- **TurboCalib** Information is persisted from HLT2 as in the Turbo stream, but the raw event information is retained and the offline reconstruction is also performed.

The TurboCalib stream, which consists exclusively of calibration selections for online monitoring and measuring PID and tracking efficiencies, is therefore suitable for the generation of calibration samples containing both HLT2-calculated and offline-calculated PID variables for each charged particle. This implies that the performance of selection requirements that include PID variables calculated in both HLT2 and offline, for example $(\mathrm{DLL}_{K\pi}^{\texttt{HLT2}} > 0)\,\&\&\,(\mathrm{DLL}_{K\pi}^{\mathrm{offline}} > 5)$, which is typical of a physics analysis using the Full stream, can straightforwardly be extracted in a data-driven way. Here $\mathrm{DLL}_{K\pi}$ is the change in $\log(\mathcal{L})$ (Delta Log-Likelihood) between the K and π hypotheses for the charged particle in question.

[1] Charge conjugation is implied except where explicitly stated

Table 1: Overview of decay modes that are used to select calibration samples. Hard (soft) refers to calibration tracks with high (low) p and p_{T}. The modes included in this table are approximately those included in the draft 2016 configuration, which is tabulated in full in Table 8.

Species	Soft	Hard
$e^{\pm}$	—	$J/\psi \to e^+e^-$
$\mu^{\pm}$	$D_s^+ \to \mu^+\mu^-\pi^+$	$J/\psi \to \mu^+\mu^-$
$\pi^{\pm}$	$K_S^0 \to \pi^+\pi^-$	$D^* \to D^0\pi^+$, $D^0 \to K^-\pi^+$
$K^{\pm}$	$D_s^+ \to K^+K^-\pi^+$	$D^* \to D^0\pi^+$, $D^0 \to K^-\pi^+$
$p^{\pm}$	$\Lambda^0 \to p\pi^-$	$\Lambda^0 \to p\pi^-$, $\Lambda_c^+ \to pK^-\pi^+$

3 Detailed description of selections

The software trigger configurations used in Run 2 that include PID calibration selections are, from the start of the EM period to the end of 2015 pp data-taking on the 4$^{\text{th}}$ November 2015, shown in Table 2. The HLT2 PID selections that were enabled in the various Trigger Configuration Keys (TCKs) are listed in Tables 6 and 7. This note also includes a draft of the 2016 configuration, which is summarised in Table 8 and listed under the fake TCK `0xDEADBEEF` throughout this note.

3.1 Trigger decorrelation

Because information from the CALO and MUON systems is included in the L0 and HLT1 triggers, care is required to ensure that the calibration samples selected in HLT2 are not

Table 2: Summary of TCKs used in 2015 with luminosity above $10\,\mathrm{nb}^{-1}$. For each TCK the corresponding version of Moore, the LHCb software trigger application, is also shown.

Era	TCK	$\mathcal{L}_{\mathrm{up}}\ [\mathrm{nb}^{-1}]$	$\mathcal{L}_{\mathrm{down}}\ [\mathrm{nb}^{-1}]$	$\mathcal{L}_{\mathrm{total}}\ [\mathrm{nb}^{-1}]$	Moore version
EM	`0x00F8014E`	0	777	777	v23r7p3
	`0x00F9014E`	124	4783	4907	v23r7p3
25 ns	`0x00FB0051`	13198	0	13198	v24r0p1
	`0x010600A2`	0	96281	96281	v24r1
	`0x010600A3`	0	60693	60693	v24r1
	`0x010600A6`	0	49	49	v24r1
	`0x010600A7`	0	1022	1022	v24r1
	`0x010700A1`	0	6355	6355	v24r1
	`0x010800A2`	49259	11380	60638	v24r2
	`0x011400A8`	73306	0	73306	v24r2

biased by the earlier trigger stages. This allows physics analyses to factorise the PID and trigger contributions to total efficiencies. In the HLT2 selections, trigger signals from L0 and HLT1 are associated with reconstructed particles. Selection requirements can therefore be made on the L0 and HLT1 trigger selections themselves, and on whether the decision was due to the signal candidate (TOS, Trigger on Signal) [6], other particles produced in the pp collision (TIS, Trigger Independent of Signal), or a combination of both.

Precisely what selection requirements are required to avoid problematic correlations depends on the mode in question, and which PID variables are to be studied. This is illustrated in the following examples:

- **Muons** Information from the MUON detectors is used in both L0 and HLT1, so the charged track used to measure PID performance is required to be TIS with respect to both L0 and HLT1. In brief, this means that the L0 and HLT1 decisions would still have been positive if the detector hits associated with the track in question were removed. The primary source of muons for the calibration samples is $J/\psi \to \mu^+\mu^-$ decay; in a typical event then the two muons will be well-separated in the MUON systems, one will be responsible for triggering L0 and HLT1 and the other will be used for calibration purposes. The selections for electrons are defined similarly.

- **Kaons** Separation of charged hadrons is largely performed by the RICH detectors. Information from these is not used in L0 or HLT1, so for some purposes it is acceptable to use kaon tracks for calibration that are not TIS with respect to L0 and HLT1. The primary source of kaons for the calibration samples is $D^{*+} \to D^0\pi^+$, $D^0 \to K^-\pi^+$ decay; in typical events the L0 will be triggered either by CALO deposits from the charged hadrons (TOS) or by other particles in the event (TIS). HLT1 will typically be triggered by one, or both, of the D^0 child particles via a selection that makes use of information from the tracking detectors only. Because for some decay modes the majority of signal candidates produced are suitable for calibration purposes, explicit requirements are not always included in the HLT2 selections. The selections for pions and protons are defined similarly to those for kaons.

The calibration samples, at present, consist exclusively of candidates selected in HLT2, so no similar decorrelation requirement is necessary for HLT2; it is sufficient to consider only L0 and HLT1. It should be noted that the requirements about the unbiased nature of the calibration samples are dependant on the variable under study. For example, at leading order the $\mathrm{DLL}_{K\pi}$ variable for kaon–pion separation relies entirely on information from the RICH detectors, so calibration tracks that are TOS and TIS at L0 are useful, despite this being correlated with the CALO values. However care must be taken with the combined PID variables, such as ProbNN [7] that combine information from the RICH, MUON, CALO and tracking detectors. It may, indeed, become necessary in some high-precision analyses to consider second order correlations. For example, the distribution of track χ^2 in tracks reconstructed in HLT2 is correlated with whether or not those tracks were TOS in HLT1. This track χ^2 is an input to the ProbNN combined PID variables, so the analysis may have to treat the PID efficiencies of tracks differently according to whether those tracks were HLT1 TOS.

3.2 Tag and probe selections

Several of the HLT2 selections are implemented according to the so-called tag and probe model. These are implemented with the same combiner classes: `LLCombiner` and `BCombiner`[2]. The lines based on this combiner have names matching the pattern `Hlt2PID.*?{Pos,Neg,OS,SS}TaggedTurboCalib`, with the `{OS,SS}Tagged` variants phased out after the EM period[3].

Taking the `DetJPsiMuMuPosTagged`[4] line as a concrete example, these tag-and-probe selections first obtain a list of well-identified, positively-charged tag tracks and a list of negatively-charged probe tracks on which the L0 and HLT1 trigger decisions were not contingent, *i.e.* TIS as defined above. These are combined to form $J/\psi \to \mu^+\mu^-$ candidates, and – because this line selects detached J/ψ candidates – these J/ψ are filtered further to form the final selection. The J/ψ candidates, before the final filtering, are re-used in the line `B2KJPsiMuMuPosTagged` where they are combined with charged kaons to form B^+ candidates.

This basic structure is reproduced for all of $J/\psi \to e^+e^-, \mu^+\mu^-, p\overline{p}$ and $\phi \to \mu^+\mu^-, K^+K^-$, where in the ϕ case the mode $D_s^+ \to \phi\pi^+$ is used in place of $B^+ \to J/\psi K^+$. Of course the entire pattern is mirrored with negatively charged tag tracks and positively charged probe tracks. Together the selections just described account for 20 of the 33 lines in the initial 25 ns configuration summarised in Table 7.

3.3 Proton selections

Proton calibration samples are obtained from two different decay modes: $\Lambda^0 \to p\pi^-$ and $\Lambda_c^+ \to pK^-\pi^+$, where the Λ_c^+ are either produced promptly or in the decay of a Λ_b^0 baryon. There are a total of eight HLT2 selections targeting these modes in the configuration used for 2015 25 ns running, four each selecting Λ^0 and Λ_c^+.

3.3.1 $\Lambda^0 \to p\pi^-$ samples

Because the visible Λ^0 production cross section in LHCb is very high, it is essential to discard a large fraction of the signal. However, some categorisation can be performed to bias the recorded candidates in a manner that improves the coverage of the sample and to this end there are four selections targeting the same decay mode. Three of these, named `Lambda2PPiLL{,highPT,veryhighPT}`, simply change the requirement on the proton transverse momentum (p_T), allowing the prescale factor[5] to be reduced for the valuable high-p_T protons. The fourth selection, `Lambda2PPiLLisMuon`, requires that

[2] "Lepton-Lepton" Combiner; in the end this was not only used for leptons. Nor is the "B" combiner only used for b-hadrons.

[3] The OS (opposite-sign) and SS (same-sign) names were misnomers; OS was subsequently corrected to Neg and SS to Pos after the end of the EM period.

[4] The `Hlt2PID` prefix and `TurboCalib` suffix will be suppressed where possible.

[5] This factor controls the fraction of events for which the selection is executed; *e.g.* a prescale of 0.1 means the selection runs on 10% of events.

the p candidate pass the `isMuonLoose` criteria, and is intended for studies of the $p \to \mu^+$ mis-identification rate.

3.3.2 $\Lambda_c^+ \to pK^-\pi^+$ samples

Due to concerns about the high-p_T phase space coverage in the Run 1 proton calibration samples, selections for Λ_c^+ decays have been included to provide complementary coverage to the Λ^0 samples. The $\Lambda_c^+ \to pK^-\pi^+$ decay mode is challenging to select with high purity without making use of RICH PID information about the p track due to, for example, the relatively low $c \to \Lambda_c^+$ hadronisation fraction and sizeable reflections from the decays $D^+ \to K^-\pi^+\pi^+$ and $D_s^+ \to K^-K^+\pi^+$. Several methods have been explored to reduce the background levels, such as only selecting the $K^*(892)^0$ mass region in $m(K^-\pi^+)$, removing events that lie in the D^+ and D_s^+ mass windows when reconstructed under alternative PID hypotheses, and using PID information about the other Λ_c^+ child tracks, K^- and π^+. Two selections reconstruct Λ_b^0 decays: `Lb2LcMuNu` (semi-muonic) and `Lb2LcPi` (hadronic), and a further two search for Λ_c^+ that are promptly produced in Σ_c decays: `Scpp2LcPi` (Σ_c^{++}) and `Sc02LcPi` (Σ_c^0). It was found that very few prompt Λ_c^+ candidates can be associated to Σ_c signals in preliminary studies of 2015 data, so these selections have been replaced with a single, prompt Λ_c^+ selection in the draft 2016 configuration.

3.4 Hadronic selections without PID requirements

The final family of selections are those that reconstruct hadronic decays without the use of PID information for any tracks[6]. The most important of these is `D02KPiTag`, which selects $D^{*+} \to D^0\pi^+$ with $D^0 \to K^-\pi^+$. This is the primary source of $K^\pm$ and $\pi^\pm$ calibration samples. In addition, `D02KPiPiPiTag` selects $D^{*+} \to D^0\pi^+$ with $D^0 \to K^-\pi^+\pi^-\pi^+$ as an alternative source of $K^\pm/\pi^\pm$ from a lower Q-value decay, `DetPhiKKUnbiased` inclusively selects $\phi \to K^+K^-$ as a source of low-p_T kaons. Finally `Ds2PiPhiKKUnbiased` reconstructs $D_s^+ \to (K^+K^-)_\phi\pi^+$, as a further source of kaons and pions, and `Ks2PiPiLL` records $K_S^0 \to \pi^+\pi^-$ (with a large prescale) to give a low-p_T, high-χ^2_{IP} pion sample. The $D^0 \to K^-\pi^+\pi^-\pi^+$ selection did not prove to be a useful source of additional kaon and pion calibration tracks, so has been removed from the draft configuration for 2016. The various $\phi \to K^+K^-$ selections that were run in 2015 with no selection requirements on PID variables were found to be too impure to be useful; in the draft 2016 configuration these have been replaced with a tag and probe $D_s^+ \to K^+K^-\pi^+$ selection.

3.5 Additional offline selection

In general, the selections implemented in HLT2 are of offline quality and are not tightened during offline analysis; in some cases the windows of invariant mass are tightened slightly before fits are performed to extract yields, while in the case of $D^0 \to K^-\pi^+$ decays, where

[6]This section excludes the previously discussed $\Lambda^0 \to p\pi^-$ samples (Sect. 3.3.1).

L0 and HLT1 requirements are not applied in the HLT2 selection, such requirements may be added offline.

4 Summary of selection performance

In this section, a brief summary is given of the signal yields and purities obtained in the 2015, 25 ns calibration samples. A small number of additional requirements are made before the yield and purity extraction takes place. These are summarised in Table 3. The additional requirements in the $B^+ \to J/\psi K^+$, $J/\psi \to e^+e^-$ channel were needed to increase the signal purity and stabilise the fit, and the draft 2016 configuration has already been modified accordingly. The additional vetoes imposed on the D_s^+ and D^0 decays will not be added to the HLT2 selections, as different choices may be required for some uses of the calibration samples. Table 4 tabulates these quantities for both magnet polarities together but split, where appropriate, by calibration track charge, while Figs. 2–14 illustrate the same information for the *MagDown* samples and one charge in each case. The signal distribution is shown by the dashed (blue) line and the background shape by the dash-dotted (green) line. It should be noted that the purity figures quoted in Table 4 are calculated over the full one or two dimensional mass variable range(s). They are not, therefore, representative of purity in the peak regions of the various distributions, but instead indicate the fraction of the HLT2 output rate that is useful signal, although no correction has been made for the efficiency of the selection requirements in Table 3. Figure 1 illustrates the improvement in proton calibration sample coverage achieved in Run 2 with the selections described in Sect. 3.3.1. In Run 1 there were two selections, with the $p < 40\,\text{GeV}/c$ region prescaled with respect to the upper region. In Run 2 the three selections have different (p_T, prescale) combinations with thresholds of 0, 3.0 and 6.0 GeV/c in p_T. The feature visible, and highlighted in the Run 2 figure, at 1.5 GeV/c corresponds to a threshold in HLT1. Above this value HLT1 can be triggered by the calibration track, while below the threshold must be triggered by some other part of the event. The kinematic coverage of the calibration samples selected in Run 2 is expected to match more closely that required for studies of b and c hadron decays.

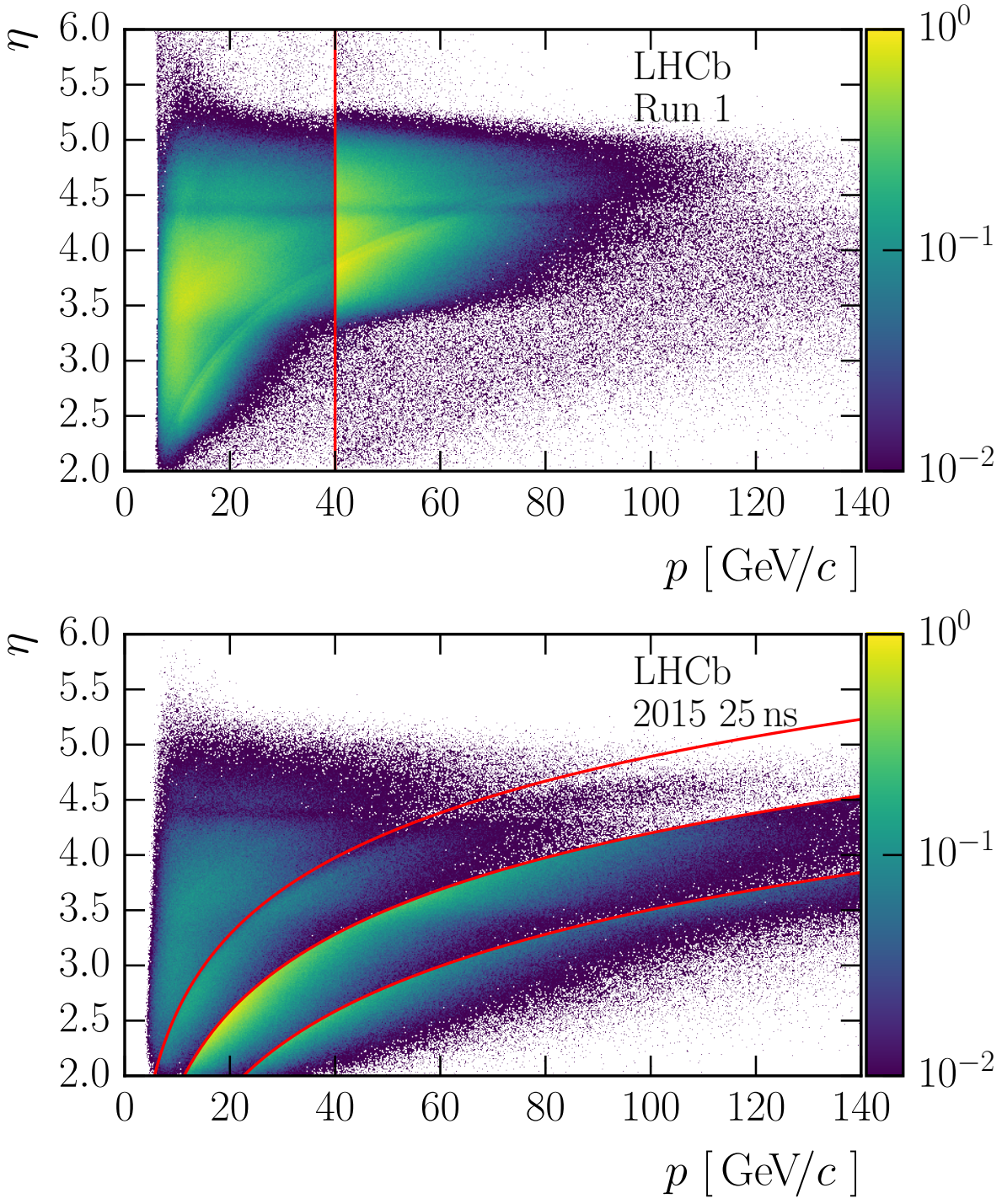

Figure 1: Distributions of proton calibration track pseudorapidity, η, and momentum, p. The upper distribution shows the coverage of the Run 1 calibration samples, with the vertical red line highlighting a boundary below which the statistics were artificially suppressed. The lower distribution shows the sample collected during the 25 ns period of data taking in 2015; the red lines correspond to $p_{\rm T}$ thresholds of 1.5, 3.0 and 6.0 GeV/c. The z-axis units are arbitrary.

Table 3: Additional selection requirements imposed offline on the 2015, 25 ns data before yield extraction fits are performed and figures produced.

Line	Offline selection
`B2KJPsiEENegTagged` `B2KJPsiEEPosTagged`	$\mathrm{B}^+ \chi^2_{\mathrm{IP}} < 9$ $\mathrm{B}^+ \chi^2_{\mathrm{vertex}}/\mathrm{ndf} < 9$ $\lvert m(\mathrm{J}/\psi\,\mathrm{K}^+) - m(\mathrm{J}/\psi) \rvert < 100\,\mathrm{MeV}/c^2$ $2250 < m(\mathrm{J}/\psi) < 3600\,\mathrm{MeV}/c^2$ $\mathrm{e}^\pm \chi^2_{\mathrm{IP}} > 25$
`D02KPiTag`	$\mathrm{D}^0 \lvert m(\mathrm{K}^- \to \pi^-, \pi^+ \to \pi^+) - m_{\mathrm{D}^0} \rvert > 25\,\mathrm{MeV}/c^2$ $\mathrm{D}^0 \lvert m(\mathrm{K}^- \to \mathrm{K}^-, \pi^+ \to \mathrm{K}^+) - m_{\mathrm{D}^0} \rvert > 25\,\mathrm{MeV}/c^2$ $\mathrm{D}^0 \lvert m(\mathrm{K}^- \to \pi^-, \pi^+ \to \mathrm{K}^+) - m_{\mathrm{D}^0} \rvert > 25\,\mathrm{MeV}/c^2$
`Ds2PiPhiKKUnbiased`	$\mathrm{D}_{\mathrm{s}}^+ \lvert m(\mathrm{K}^+ \to \pi^+, \mathrm{K}^- \to \mathrm{K}^-, \pi^+ \to \pi^+) - 1860\,\mathrm{MeV}/c^2 \rvert > 30\,\mathrm{MeV}/c^2$ $\mathrm{D}_{\mathrm{s}}^+ \lvert m(\mathrm{K}^+ \to \mathrm{p}, \mathrm{K}^- \to \mathrm{K}^-, \pi^+ \to \pi^+) - 2286\,\mathrm{MeV}/c^2 \rvert > 20\,\mathrm{MeV}/c^2$

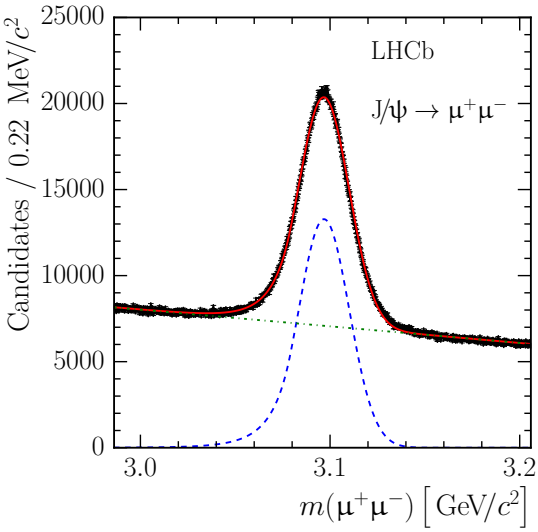

Figure 2: `DetJPsiMuMuPosTagged` invariant mass distribution in 2015, *MagDown*, 25 ns data

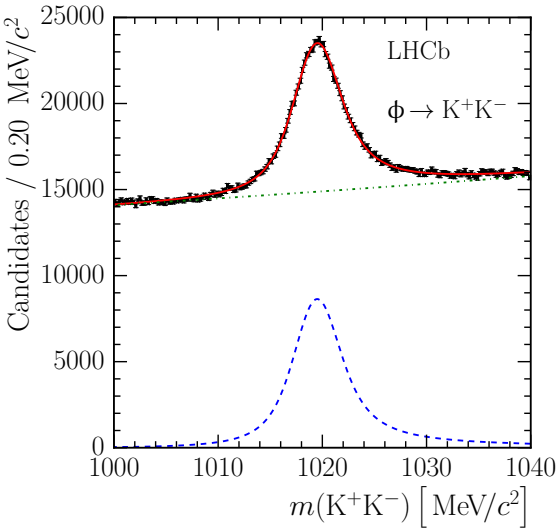

Figure 3: `DetPhiKKPosTagged` invariant mass distribution in 2015, *MagDown*, 25 ns data

Table 4: Yield and purity summary in the 2015, 25 ns data sample. Only statistical uncertainties are quoted.

Line	Signal [$\times 10^3$]	Purity [%]
B2KJPsiEENegTagged	13.44 ± 0.13	57.93 ± 0.22
B2KJPsiEEPosTagged	13.33 ± 0.13	57.94 ± 0.22
B2KJPsiMuMuNegTagged	90.29 ± 0.31	60.00 ± 0.06
B2KJPsiMuMuPosTagged	90.81 ± 0.32	60.34 ± 0.06
D02KPiPiPiTag π^-	1251.2 ± 1.6	15.203 ± 0.014
D02KPiPiPiTag π^+	1133.6 ± 1.5	13.744 ± 0.012
D02KPiTag π^-	20004 ± 5	68.364 ± 0.010
D02KPiTag π^+	19582 ± 5	67.805 ± 0.010
DetJPsiMuMuNegTagged	3469.2 ± 2.8	22.552 ± 0.014
DetJPsiMuMuPosTagged	3488.1 ± 2.8	22.924 ± 0.014
DetPhiKKNegTagged	520.8 ± 1.7	10.481 ± 0.032
DetPhiKKPosTagged	522.7 ± 1.8	9.851 ± 0.031
Ds2PiPhiKKNegTagged	4492.7 ± 2.7	52.991 ± 0.019
Ds2PiPhiKKPosTagged	4491.4 ± 2.6	52.613 ± 0.018
Ds2PiPhiKKUnbiased	6488.5 ± 3.2	28.498 ± 0.008
Ks2PiPiLL	8889.9 ± 3.4	74.565 ± 0.013
Lambda2PPiLLhighPT p^+	11020.5 ± 3.4	96.446 ± 0.007
Lambda2PPiLLhighPT p^-	10776.3 ± 3.4	96.335 ± 0.007
Lambda2PPiLLveryhighPT p^+	3552.9 ± 2.0	86.100 ± 0.016
Lambda2PPiLLveryhighPT p^-	3274.1 ± 1.9	86.072 ± 0.017
Lambda2PPiLL p^+	7145.2 ± 2.8	93.757 ± 0.009
Lambda2PPiLL p^-	6758.5 ± 2.7	93.121 ± 0.010
Lb2LcMuNu	149.1 ± 0.5	17.61 ± 0.04

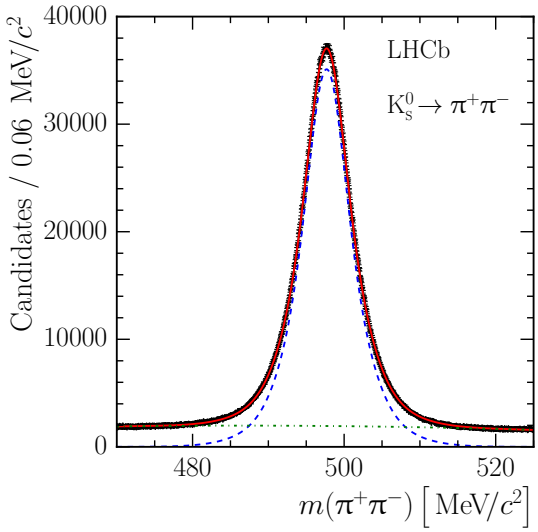

Figure 4: `Ks2PiPiLL` invariant mass distribution in 2015, *MagDown*, 25 ns data

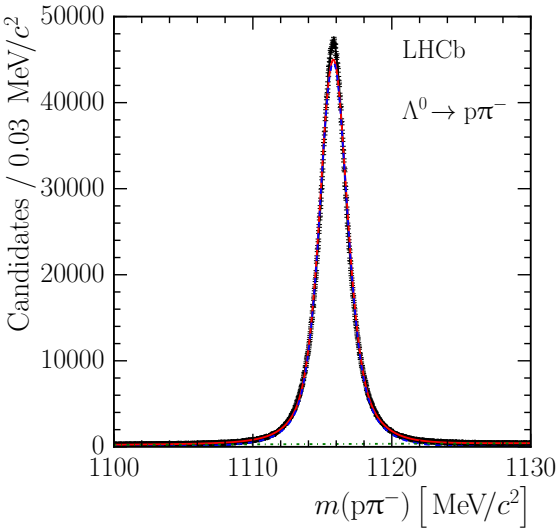

Figure 5: `Lambda2PPiLL` invariant mass distribution in 2015, *MagDown*, 25 ns data

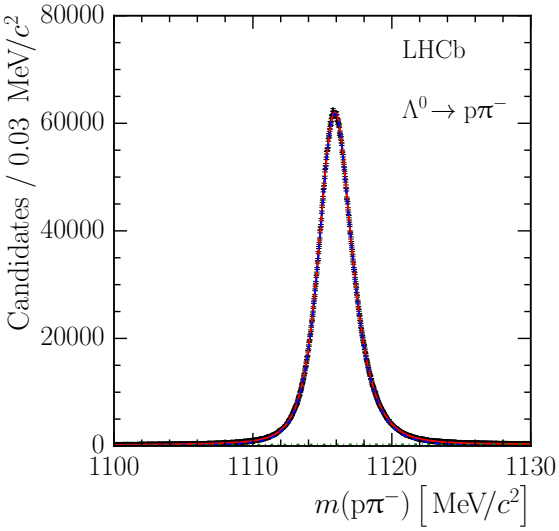

Figure 6: `Lambda2PPiLLhighPT` invariant mass distribution in 2015, *MagDown*, 25 ns data

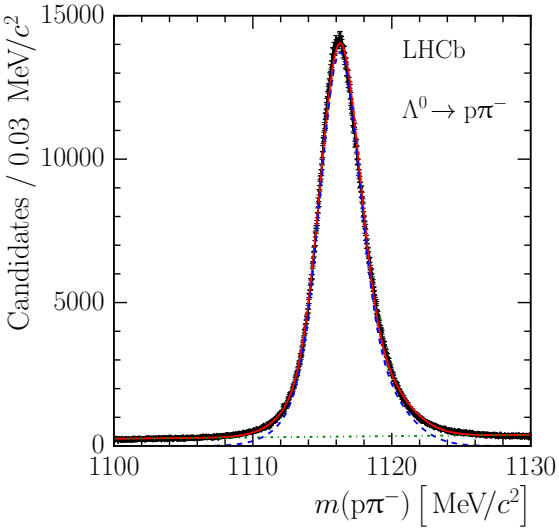

Figure 7: `Lambda2PPiLLveryhighPT` invariant mass distribution in 2015, *MagDown*, 25 ns data

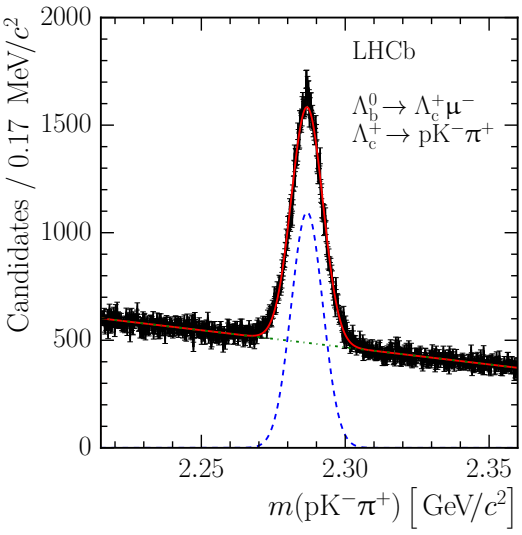

Figure 8: `Lb2LcMuNu` invariant mass distribution in 2015, *MagDown*, 25 ns data

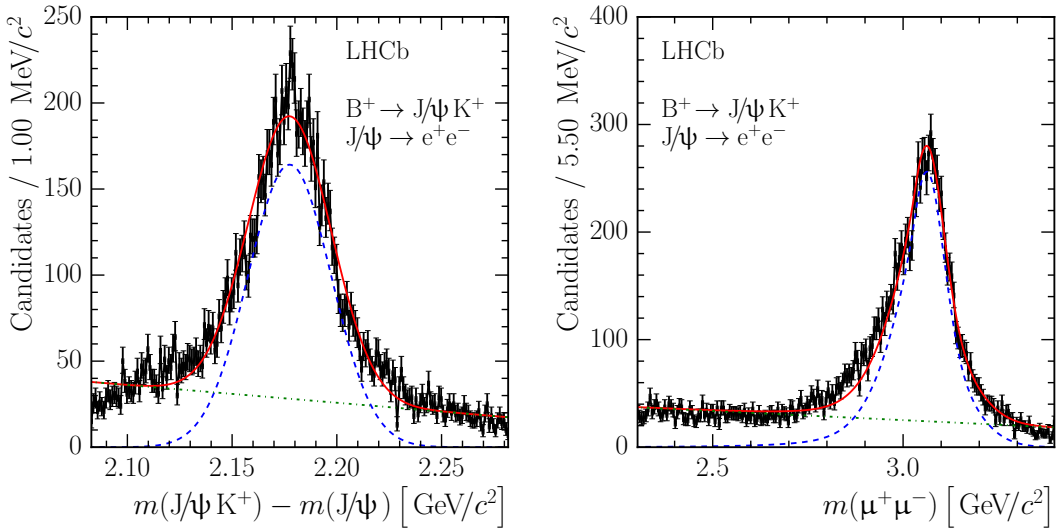

Figure 9: `B2KJPsiEEPosTagged` invariant mass distributions in 2015, *MagDown*, 25 ns data

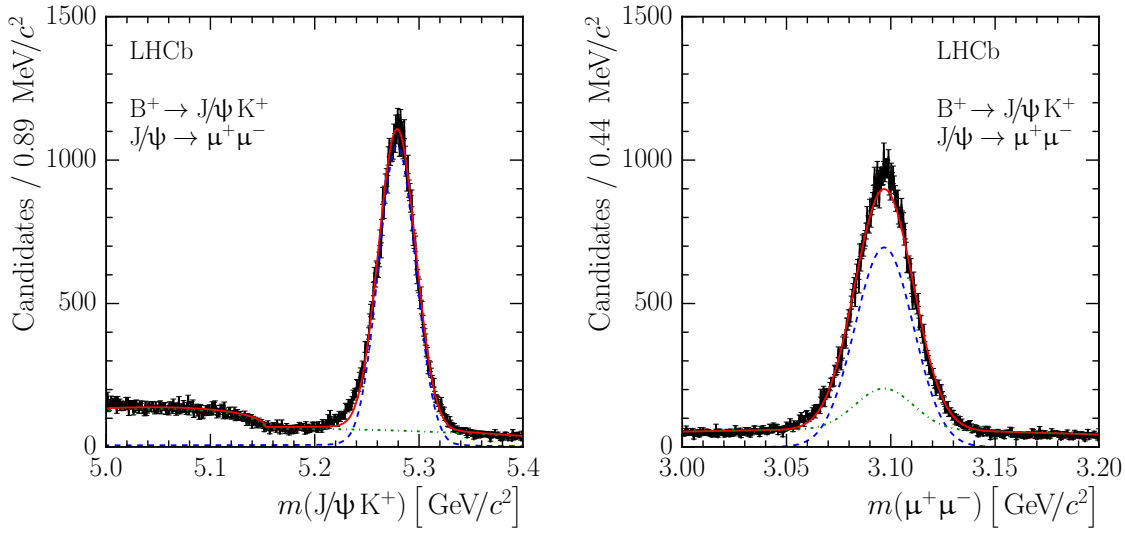

Figure 10: `B2KJPsiMuMuPosTagged` invariant mass distributions in 2015, *MagDown*, 25 ns data

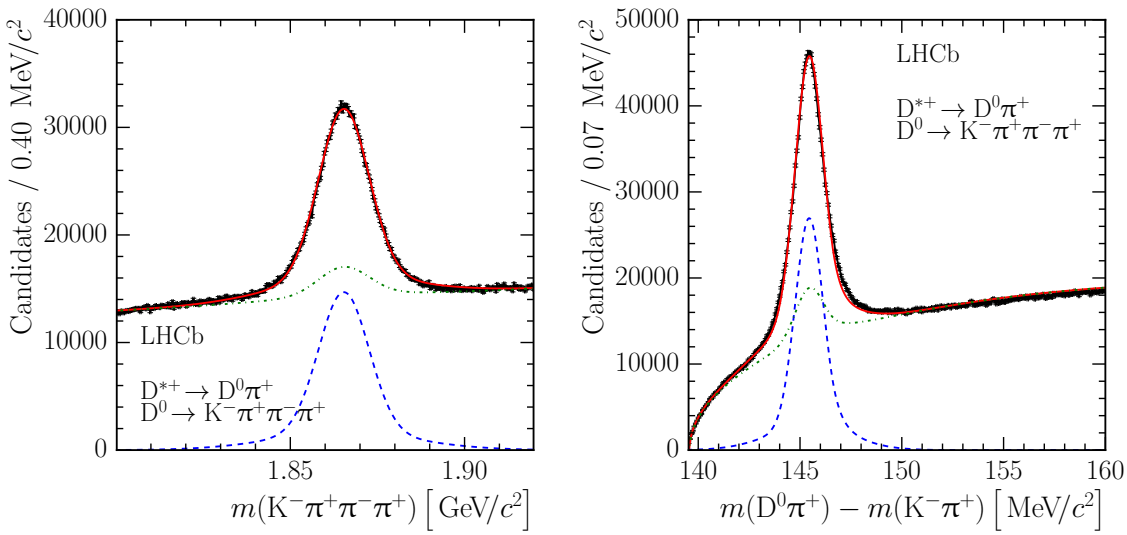

Figure 11: `D02KPiPiPiTag` invariant mass distributions in 2015, *MagDown*, 25 ns data

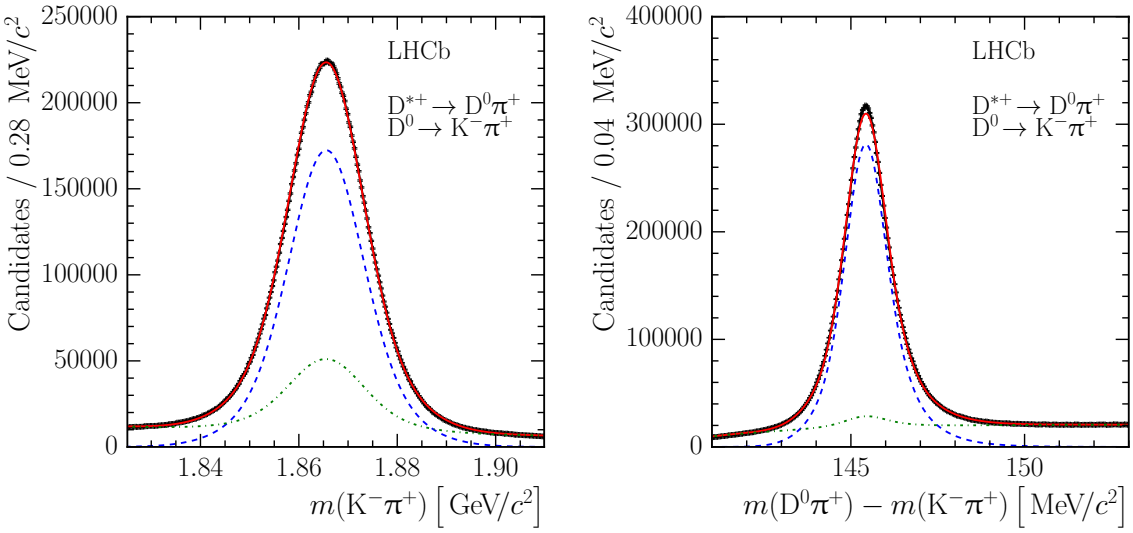

Figure 12: `D02KPiTag` invariant mass distributions in 2015, *MagDown*, 25 ns data

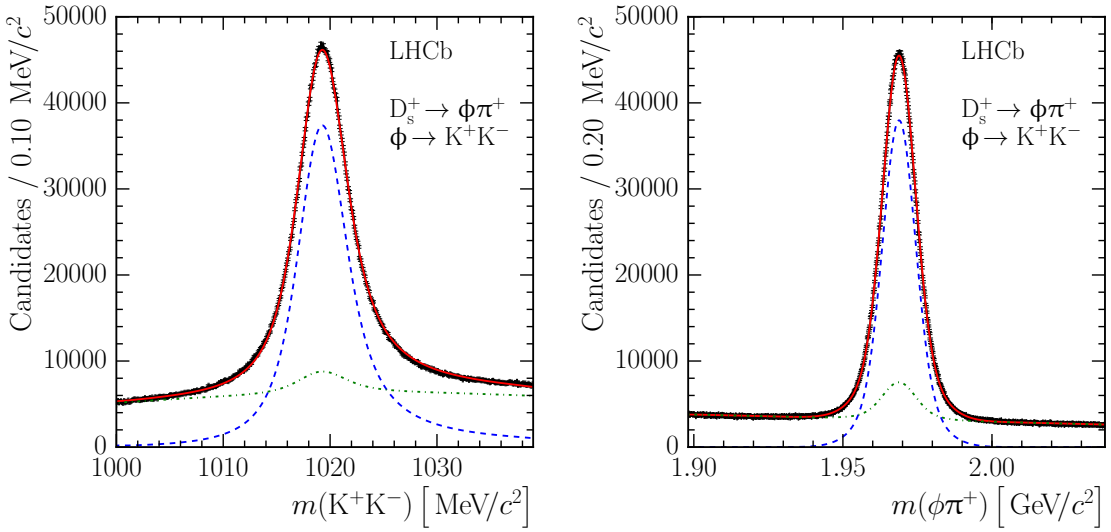

Figure 13: `Ds2PiPhiKKPosTagged` invariant mass distributions in 2015, *MagDown*, 25 ns data

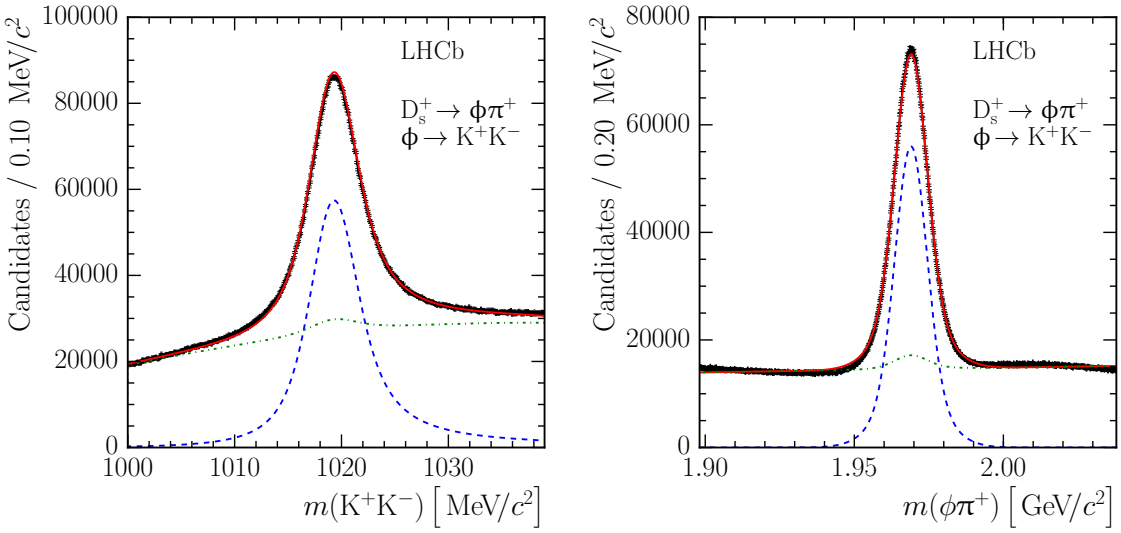

Figure 14: `Ds2PiPhiKKUnbiased` invariant mass distributions in 2015, *MagDown*, 25 ns data

5 Conclusions

The strategy for the selection of PID calibration samples has seen large changes for Run 2 of the LHC. The samples are now selected directly in HLT2, which has several benefits with respect to the offline sample selection used in Run 1. New calibration modes and selections have been included that improve the kinematic coverage of the calibration samples, for example boosting the high-p_{T} proton samples using dedicated $\Lambda^0 \to \mathrm{p}\pi^-$ selections. These samples are used for data-driven measurement of PID performance and monitoring of the detectors that contribute information to the PID variables. The description of these tools is beyond the scope of this note; the analysis tools come under the umbrella of the PIDCalib package, this is described in more detail in Ref. [8], which is currently in preparation.

References

[1] LHCb collaboration, A. A. Alves Jr. *et al.*, *The LHCb detector at the LHC*, JINST **3** (2008) S08005.

[2] R. Aaij *et al.*, *Performance of the LHCb full real-time reconstruction and high-level trigger with 13 TeV data*, in preparation.

[3] R. Aaij *et al.*, *The novel real-time alignment and calibration of the LHCb detector*, in preparation.

[4] B. Sciascia *et al.*, *Computing and selection strategy for PID calibration samples for LHCb Run-II*, Tech. Rep. LHCb-INT-2015-016. CERN-LHCb-INT-2015-016, CERN, Geneva, May, 2015.

[5] R. Aaij *et al.*, *Tesla: an application for real-time data analysis in High Energy Physics*, in preparation.

[6] R. Aaij *et al.*, *The LHCb trigger and its performance in 2011*, JINST **8** (2013) P04022, `arXiv:1211.3055`.

[7] LHCb collaboration, R. Aaij *et al.*, *LHCb detector performance*, Int. J. Mod. Phys. **A30** (2015) 1530022, `arXiv:1412.6352`.

[8] A. Pearce *et al.*, *The PIDCalib package*, LHCb-PUB-2016-XXX in preparation.

Appendix

The appendix contains detailed descriptions of the PID calibration samples used during 2015 data-taking, and includes the draft configuration for 2016 under the fake TCK `0xDEADBEEF`. Table 5 defines various symbols and nomenclature used throughout the appendix. The next three tables summarise the HLT2 selections and prescales that were used. Table 6 shows the configuration used during the EM period of data-taking with 50 ns bunch spacing in 2015. Table 7 lists the configuration used for data-taking with 25 ns bunch spacing, and finally Table 8 shows the draft configuration for 2016.

The remaining tables in this document list the various selection requirements that are used. The text will not explicitly refer to each of them, but some illustrative examples are explained here. Each selection listed in Tables 6–8 has a corresponding table listing its content, for example the selection `Hlt2PIDDetJPsiEEPosTaggedTurboCalib` in the configurations `0x00FB0051`, `0x0106XXXX`, `0x010700A1`, `0x010800A2` and `0x011400A8` (summarised in Table 7) is described in Table 9. This is describing a simple $J/\psi \to e^+e^-$ selection; the first section lists selection requirements on the negatively charged electron, the second section lists those applying to the positively charged electron, the third section shows requirements that are applied to the e^+e^- combination before the vertex fit has been carried out, and the final section of the table shows requirements that are evaluated using the vertexed J/ψ candidate. Some tables have been omitted when they would be trivially related to others, for instance there is no table describing `Hlt2PIDDetJPsiEENegTaggedTurboCalib` because it would be near-identical to that describing `Hlt2PIDDetJPsiEEPosTaggedTurboCalib` (Table 9). In some cases, selections are more complex and their description is split across multiple tables. For example, Table 30 describes a $B^+ \to J/\psi K^+$ selection that takes J/ψ candidates from an external location (`Hlt2/Hlt2PIDJPsiEEPosTaggedCombiner`). The table caption includes cross-references to Tables 50 and 51, which describe the J/ψ selection. In some cases, such as Tables 55 and 56, multiple tables exist that are very similar. In this case the difference is that one set of Λ_c^+ candidates is used as input for Λ_b^0 selections and in the other case the Λ_c^+ candidates are used to produce Σ_c; this is apparent from the table captions describing the top-level selections. Note that this does not imply that the computation time used to combine and vertex-fit Λ_c^+ candidates is duplicated. Finally, to allow the configurations to be listed more compactly, ranges of TCKs such as `0x010600A2`, `0x010600A3`, `0x010600A6` and `0x010600A7` are denoted by `0x0106XXXX`, where the final four characters only govern the L0 configuration, which is not relevant for the PID selections.

Table 5: Definitions of the various symbols used throughout the appendix to tabulate selection requirements.

Variable	Description
p	Modulus of 3-momentum, $\|\vec{p}\|$.
p_{T}	Component of p transverse to the beam line.
m	Invariant mass.
m_X	Known mass of particle X.
$m(x \to y, ...)$	Invariant mass evaluated using the alternative mass hypothesis y for child x.
$m_{\mathrm{corr.}}$	Corrected mass. Given by $\sqrt{m^2 + \|p'_{T\,\mathrm{miss}}\|^2} + \|p'_{T\,\mathrm{miss}}\|$, this is the minimal mass of the parent if a massless particle was omitted from the reconstructed candidate [6].
χ^2_{IP}	Increase in χ^2 of a primary vertex if the particle in question was added to the vertex.
χ^2_{track}/ndf	χ^2 per degree of freedom from the track fit.
χ^2_{VS}	χ^2 separation of the decay vertex of a particle from the primary vertex that it is associated with.
DOCA(x, y)	Distance of closest approach of particles x and y.
$\chi^2_{\mathrm{DOCA}}(x, y)$	χ^2 significance of DOCA(x, y).
χ^2_{vertex}	χ^2 of the vertex fit.
χ^2_{vertex}/ndf	χ^2 per degree of freedom of the vertex fit.
z_{vertex}	Vertex position in the z coordinate. The positive z-axis is parallel to the beam line and extends from its origin in the Vertex Locator towards the MUON stations.
DIRA$_{\mathrm{PV}}$	Cosine of the angle between the reconstructed particle momentum and the displacement vector connecting its decay vertex and associated primary vertex.
τ	Proper decay time evaluated with respect to the associated primary vertex.
Long track	Track traverses the full LHCb tracking system.
IsMuon	Track has a, momentum dependent, minimum number of hits in the MUON stations around its extrapolated position.
IsMuonLoose	Alternative version of IsMuon with looser hit requirements.
DLL$_{xy}$	Change in $\log(\mathcal{L})$ (Delta Log-Likelihood) between the x and y particle mass hypotheses given information from the RICH, CALO and MUON systems.
GhostProb	Multivariate classifier that separates genuine and ghost tracks using several inputs from the tracking algorithms [2].
Has{Calo, Muon,Rich}	Particle has information from the sub-detector in question, *i.e.* it is in the appropriate geometric acceptance.
NumChildren(X)	The number of child particles satisfying requirement X.

Table 6: Overview of HLT2 PID lines for TCKs `0x00F8014E` and `0x00F9014E`: the EM configuration.

HLT2 line	Prescale	Postscale
`Hlt2PIDB2KJPsiEEOSTaggedTurboCalib`	1	1
`Hlt2PIDB2KJPsiEESSTaggedTurboCalib`	1	1
`Hlt2PIDD02KPiTagTurboCalib`	1	1
`Hlt2PIDDetJPsiMuMuNegTaggedTurboCalib`	1	1
`Hlt2PIDDetJPsiMuMuPosTaggedTurboCalib`	1	1
`Hlt2PIDLambda2PPiLLTurboCalib`	0.003	1
`Hlt2PIDLambda2PPiLLhighPTTurboCalib`	0.1	1
`Hlt2PIDLambda2PPiLLisMuonTurboCalib`	0.05	1
`Hlt2PIDLambda2PPiLLveryhighPTTurboCalib`	1	1
`Hlt2PIDLb2LcMuNuTurboCalib`	1	1
`Hlt2PIDLb2LcPiTurboCalib`	1	1

Table 7: Overview of HLT2 PID lines for TCKs `0x00FB0051`, `0x0106XXXX`, `0x010700A1`, `0x010800A2` and `0x011400A8`: the 2015, 25 ns configuration.

HLT2 line	Prescale	Postscale
Hlt2PIDB2KJPsiEENegTaggedTurboCalib	1	1
Hlt2PIDB2KJPsiEEPosTaggedTurboCalib	1	1
Hlt2PIDB2KJPsiMuMuNegTaggedTurboCalib	1	1
Hlt2PIDB2KJPsiMuMuPosTaggedTurboCalib	1	1
Hlt2PIDB2KJPsiPPNegTaggedTurboCalib	1	1
Hlt2PIDB2KJPsiPPPosTaggedTurboCalib	1	1
Hlt2PIDD02KPiPiPiTagTurboCalib	0.1	1
Hlt2PIDD02KPiTagTurboCalib	1	1
Hlt2PIDDetJPsiEENegTaggedTurboCalib	0.01	1
Hlt2PIDDetJPsiEEPosTaggedTurboCalib	0.01	1
Hlt2PIDDetJPsiMuMuNegTaggedTurboCalib	1	1
Hlt2PIDDetJPsiMuMuPosTaggedTurboCalib	1	1
Hlt2PIDDetJPsiPPNegTaggedTurboCalib	0.01	1
Hlt2PIDDetJPsiPPPosTaggedTurboCalib	0.01	1
Hlt2PIDDetPhiKKNegTaggedTurboCalib	0.005	1
Hlt2PIDDetPhiKKPosTaggedTurboCalib	0.005	1
Hlt2PIDDetPhiKKUnbiasedTurboCalib	0.001	1
Hlt2PIDDetPhiMuMuNegTaggedTurboCalib	0.1	1
Hlt2PIDDetPhiMuMuPosTaggedTurboCalib	0.1	1
Hlt2PIDDs2PiPhiKKNegTaggedTurboCalib	1	1
Hlt2PIDDs2PiPhiKKPosTaggedTurboCalib	1	1
Hlt2PIDDs2PiPhiKKUnbiasedTurboCalib	1	1
Hlt2PIDDs2PiPhiMuMuNegTaggedTurboCalib	1	1
Hlt2PIDDs2PiPhiMuMuPosTaggedTurboCalib	1	1
Hlt2PIDKs2PiPiLLTurboCalib	0.0005	1
Hlt2PIDLambda2PPiLLTurboCalib	0.003	1
Hlt2PIDLambda2PPiLLhighPTTurboCalib	0.1	1
Hlt2PIDLambda2PPiLLisMuonTurboCalib	0.05	1
Hlt2PIDLambda2PPiLLveryhighPTTurboCalib	1	1
Hlt2PIDLb2LcMuNuTurboCalib	1	1
Hlt2PIDLb2LcPiTurboCalib	1	1
Hlt2PIDSc02LcPiTurboCalib	1	1
Hlt2PIDScpp2LcPiTurboCalib	1	1

Table 8: Overview of HLT2 PID lines for TCK `0xDEADBEEF`: the draft 2016 configuration.

HLT2 line	Prescale	Postscale
`Hlt2PIDB2KJPsiEENegTaggedTurboCalib`	1	1
`Hlt2PIDB2KJPsiEEPosTaggedTurboCalib`	1	1
`Hlt2PIDB2KJPsiMuMuNegTaggedTurboCalib`	1	1
`Hlt2PIDB2KJPsiMuMuPosTaggedTurboCalib`	1	1
`Hlt2PIDD02KPiTagTurboCalib`	1	1
`Hlt2PIDDetJPsiMuMuNegTaggedTurboCalib`	1	1
`Hlt2PIDDetJPsiMuMuPosTaggedTurboCalib`	1	1
`Hlt2PIDDs2KKPiSSTaggedTurboCalib`	0.5	1
`Hlt2PIDDs2MuMuPiNegTaggedTurboCalib`	0.05	1
`Hlt2PIDDs2MuMuPiPosTaggedTurboCalib`	0.05	1
`Hlt2PIDKs2PiPiLLTurboCalib`	0.0005	1
`Hlt2PIDLambda2PPiLLTurboCalib`	0.003	1
`Hlt2PIDLambda2PPiLLhighPTTurboCalib`	0.1	1
`Hlt2PIDLambda2PPiLLisMuonTurboCalib`	0.05	1
`Hlt2PIDLambda2PPiLLveryhighPTTurboCalib`	1	1
`Hlt2PIDLb2LcMuNuTurboCalib`	1	1
`Hlt2PIDLb2LcPiTurboCalib`	1	1
`Hlt2PIDLc2KPPiTurboCalib`	1	1

Table 9: Description of `Hlt2PIDDetJPsiEEPosTaggedTurboCalib` for TCKs `0x00FB0051`, `0x0106XXXX`, `0x010700A1`, `0x010800A2` and `0x011400A8`: the 2015, 25 ns configuration. This combines $J/\psi \to e^+e^-$.

e^-	$\chi^2_{IP} > 9$, $p_T > 500\,\text{MeV}/c$, $p > 3000\,\text{MeV}/c$, charge < 0 $\chi^2_{track}/\text{ndf} < 5$, `Hlt1.*Decision TIS`, long track `L0(Photon|Electron|Hadron|Muon|DiMuon)Decision TIS`
e^+	$\chi^2_{IP} > 25$, $\text{DLL}_{e\pi} > 5$, $p_T > 1500\,\text{MeV}/c$, $p > 6000\,\text{MeV}/c$ GhostProb < 1, charge > 0, $\chi^2_{track}/\text{ndf} < 5$, HasCalo long track
e^+e^-	$\chi^2_{DOCA}(e^+, e^-) < 18$, $\lvert m - 2896\,\text{MeV}/c^2\rvert < 710\,\text{MeV}/c^2$
J/ψ	$\chi^2_{IP} > 15$, $\chi^2_{VS} > 100$, $p_T > 2000\,\text{MeV}/c$ $\text{DIRA}_{PV} > 0.99$, $\chi^2_{vertex} < 9$, $\lvert m - 2896\,\text{MeV}/c^2\rvert < 700\,\text{MeV}/c^2$

Table 10: Description of `Hlt2PIDDetJPsiMuMuPosTaggedTurboCalib` for TCKs `0x00F8014E` and `0x00F9014E`: the EM configuration. This combines $J/\psi \to \mu^+\mu^-$.

μ^-	$\chi^2_{\rm IP} > 16$, $p_{\rm T} > 500\,{\rm MeV}/c$, $p > 3000\,{\rm MeV}/c$, charge < 0 $\chi^2_{\rm track}/{\rm ndf} < 5$, long track
μ^+	IsMuon, $\chi^2_{\rm IP} > 9$, $p_{\rm T} > 1200\,{\rm MeV}/c$, $p > 3000\,{\rm MeV}/c$ charge > 0, $\chi^2_{\rm track}/{\rm ndf} < 3$, HasMuon, long track
$\mu^+\mu^-$	$\chi^2_{\rm DOCA}(\mu^+, \mu^-) < 10$, $\lvert m - 3096\,{\rm MeV}/c^2\rvert < 210\,{\rm MeV}/c^2$
J/ψ	$\chi^2_{\rm IP} > 5$, $\chi^2_{\rm VS} > 50$, $p_{\rm T} > 1000\,{\rm MeV}/c$, $\chi^2_{\rm vertex} < 15$ $\lvert m - 3096\,{\rm MeV}/c^2\rvert < 200\,{\rm MeV}/c^2$

Table 11: Description of `Hlt2PIDDetJPsiMuMuPosTaggedTurboCalib` for TCKs `0x00FB0051`, `0x0106XXXX`, `0x010700A1`, `0x010800A2` and `0x011400A8`: the 2015, 25 ns configuration. This combines $J/\psi \to \mu^+\mu^-$.

μ^-	$\chi^2_{\rm IP} > 9$, $p_{\rm T} > 0\,{\rm MeV}/c$, $p > 3000\,{\rm MeV}/c$, charge < 0 $\chi^2_{\rm track}/{\rm ndf} < 5$, `L0(Muon|DiMuon)Decision TIS`, long track `Hlt1(TrackAllL0|TrackMuon|SingleMuon|DiMuon|TrackMVA|TwoTrackMVA).*Decision TIS`
μ^+	IsMuon, $\chi^2_{\rm IP} > 9$, $p_{\rm T} > 1200\,{\rm MeV}/c$, $p > 3000\,{\rm MeV}/c$ GhostProb < 0.2, charge > 0, $\chi^2_{\rm track}/{\rm ndf} < 3$, HasMuon long track
$\mu^+\mu^-$	$\chi^2_{\rm DOCA}(\mu^+, \mu^-) < 10$, $\lvert m - 3096\,{\rm MeV}/c^2\rvert < 210\,{\rm MeV}/c^2$
J/ψ	$\chi^2_{\rm IP} > 5$, $\chi^2_{\rm VS} > 150$, $p_{\rm T} > 1000\,{\rm MeV}/c$ ${\rm DIRA}_{\rm PV} > 0.995$, $\chi^2_{\rm vertex} < 15$, $\lvert m - 3096\,{\rm MeV}/c^2\rvert < 200\,{\rm MeV}/c^2$

Table 12: Description of `Hlt2PIDDetJPsiMuMuPosTaggedTurboCalib` for TCK `0xDEADBEEF`: the draft 2016 configuration. This combines $J/\psi \to \mu^+\mu^-$.

μ^-	$\chi^2_{\rm IP} > 20$, $p_{\rm T} > 0\,{\rm MeV}/c$, $p > 3000\,{\rm MeV}/c$, charge < 0 $\chi^2_{\rm track}/{\rm ndf} < 4$, `Hlt1.*Decision TIS` `L0(Muon|DiMuon)Decision TIS`, long track
μ^+	IsMuon, $\chi^2_{\rm IP} > 9$, $p_{\rm T} > 1200\,{\rm MeV}/c$, $p > 3000\,{\rm MeV}/c$ GhostProb < 0.2, charge > 0, $\chi^2_{\rm track}/{\rm ndf} < 4$, HasMuon long track
$\mu^+\mu^-$	$\chi^2_{\rm DOCA}(\mu^+, \mu^-) < 5$, $\lvert m - 3071\,{\rm MeV}/c^2\rvert < 185\,{\rm MeV}/c^2$
J/ψ	$\chi^2_{\rm IP} > 5$, $\chi^2_{\rm VS} > 150$, $p_{\rm T} > 1000\,{\rm MeV}/c$ ${\rm DIRA}_{\rm PV} > 0.995$, $\chi^2_{\rm vertex} < 15$, $\lvert m - 3071\,{\rm MeV}/c^2\rvert < 175\,{\rm MeV}/c^2$

Table 13: Description of `Hlt2PIDDetJPsiPPPosTaggedTurboCalib` for TCKs `0x00FB0051`, `0x0106XXXX`, `0x010700A1`, `0x010800A2` and `0x011400A8`: the 2015, 25 ns configuration. This combines $J/\psi \to p\overline{p}$.

p	$\chi^2_{\rm IP} > 25$, ${\rm DLL}_{p\pi} > 5$, $p_{\rm T} > 1500\,{\rm MeV}/c$, $p > 3000\,{\rm MeV}/c$ GhostProb < 0.2, charge > 0, $\chi^2_{\rm track}/{\rm ndf} < 3$, HasRich long track
$\overline{p}$	$\chi^2_{\rm IP} > 16$, $p_{\rm T} > 800\,{\rm MeV}/c$, $p > 3000\,{\rm MeV}/c$, charge < 0 $\chi^2_{\rm track}/{\rm ndf} < 5$, long track
$p\overline{p}$	$\chi^2_{\rm DOCA}(p, \overline{p}) < 10$, $\lvert m - 3096\,{\rm MeV}/c^2\rvert < 220\,{\rm MeV}/c^2$
J/ψ	$\chi^2_{\rm IP} > 5$, $\chi^2_{\rm VS} > 150$, $p_{\rm T} > 1000\,{\rm MeV}/c$ ${\rm DIRA}_{\rm PV} > 0.995$, $\chi^2_{\rm vertex} < 15$, $\lvert m - 3096\,{\rm MeV}/c^2\rvert < 200\,{\rm MeV}/c^2$

Table 14: Description of `Hlt2PIDDetPhiKKPosTaggedTurboCalib` for TCKs `0x00FB0051`, `0x0106XXXX`, `0x010700A1`, `0x010800A2` and `0x011400A8`: the 2015, 25 ns configuration. This combines $\phi \to K^+K^-$.

K^+	$\chi^2_{IP} > 16$, $DLL_{K\pi} > 0$, $p_T > 200\,MeV/c$, $p > 3000\,MeV/c$ GhostProb < 0.2, charge > 0, $\chi^2_{track}/ndf < 3$, HasRich long track
K^-	$\chi^2_{IP} > 9$, $p_T > 0\,MeV/c$, $p > 3000\,MeV/c$, charge < 0 $\chi^2_{track}/ndf < 5$, long track
K^+K^-	$\chi^2_{DOCA}(K^+, K^-) < 15$, $\lvert m - 1020\,MeV/c^2\rvert < 40\,MeV/c^2$
ϕ	$\chi^2_{IP} > 25$, $\chi^2_{VS} > 150$, $p_T > 200\,MeV/c$ $DIRA_{PV} > 0.99$, $\chi^2_{vertex} < 15$, $\lvert m - 1020\,MeV/c^2\rvert < 20\,MeV/c^2$

Table 15: Description of `Hlt2PIDDetPhiKKUnbiasedTurboCalib` for TCKs `0x00FB0051`, `0x0106XXXX`, `0x010700A1`, `0x010800A2` and `0x011400A8`: the 2015, 25 ns configuration. This combines $\phi \to K^+K^-$.

K^+	$\chi^2_{IP} > 16$, $p_T > 0\,MeV/c$
K^+K^-	$\chi^2_{DOCA}(K^+, K^-) < 15$, $p_T(K^+) + p_T(K^-) > 200\,MeV/c$ NumChildren($\chi^2_{IP} > 40$) ≥ 1 NumChildren($p_T > 200\,MeV/c$) ≥ 1, $\lvert m - m_\phi\rvert < 40\,MeV/c^2$
ϕ	$\chi^2_{IP} > 25$, $\chi^2_{VS} > 150$, $p_T > 800\,MeV/c$ $DIRA_{PV} > 0.995$, $\chi^2_{vertex} < 15$, $\lvert m - m_\phi\rvert < 20\,MeV/c^2$

Table 16: Description of `Hlt2PIDDetPhiMuMuPosTaggedTurboCalib` for TCKs `0x00FB0051`, `0x0106XXXX`, `0x010700A1`, `0x010800A2` and `0x011400A8`: the 2015, 25 ns configuration. This combines $\phi \to \mu^+\mu^-$.

μ^-	$\chi^2_{\rm IP} > 9$, $p_{\rm T} > 0\,{\rm MeV}/c$, $p > 3000\,{\rm MeV}/c$, charge < 0 $\chi^2_{\rm track}/{\rm ndf} < 5$, `L0(Muon|DiMuon)Decision TIS`, long track `Hlt1(TrackAllL0|TrackMuon|SingleMuon|DiMuon|TrackMVA|TwoTrackMVA).*Decision TIS`
μ^+	IsMuon, $\chi^2_{\rm IP} > 25$, $p_{\rm T} > 500\,{\rm MeV}/c$, $p > 3000\,{\rm MeV}/c$ GhostProb < 0.2, charge > 0, $\chi^2_{\rm track}/{\rm ndf} < 3$, HasMuon long track
$\mu^+\mu^-$	$\chi^2_{\rm DOCA}(\mu^+, \mu^-) < 9$, $\lvert m - 1020\,{\rm MeV}/c^2\rvert < 40\,{\rm MeV}/c^2$
ϕ	$\chi^2_{\rm IP} > 15$, $\chi^2_{\rm VS} > 100$, $p_{\rm T} > 800\,{\rm MeV}/c$ ${\rm DIRA}_{\rm PV} > 0.99$, $\chi^2_{\rm vertex} < 15$, $\lvert m - 1020\,{\rm MeV}/c^2\rvert < 25\,{\rm MeV}/c^2$

Table 17: Description of `Hlt2PIDDs2KKPiSSTaggedTurboCalib` for TCK `0xDEADBEEF`: the draft 2016 configuration. This combines $D_s^- \to K^-K^+\pi^-$.

K^+	$\chi^2_{\rm IP} > 9$, $p_{\rm T} > 200\,{\rm MeV}/c$, $p > 1000\,{\rm MeV}/c$, charge > 0 $\chi^2_{\rm track}/{\rm ndf} < 3$, long track
π^+	$\chi^2_{\rm IP} > 9$, $p_{\rm T} > 200\,{\rm MeV}/c$, $p > 1000\,{\rm MeV}/c$, $\chi^2_{\rm track}/{\rm ndf} < 3$
K^-	$\chi^2_{\rm IP} > 16$, ${\rm DLL}_{K\pi} > 0$, $p_{\rm T} > 400\,{\rm MeV}/c$, $p > 3000\,{\rm MeV}/c$ GhostProb < 0.2, charge < 0, $\chi^2_{\rm track}/{\rm ndf} < 3$, long track
$K^-K^+\pi^-$	$p_{\rm T}(K^-) + p_{\rm T}(K^+) + p_{\rm T}(\pi^-) > 2000\,{\rm MeV}/c$ NumChildren($\chi^2_{\rm IP} > 20$) ≥ 2 NumChildren($\chi^2_{\rm IP} > 40$) ≥ 1 NumChildren($p_{\rm T} > 200\,{\rm MeV}/c$) ≥ 2 NumChildren($p_{\rm T} > 400\,{\rm MeV}/c$) ≥ 1, $\lvert m - 1968\,{\rm MeV}/c^2\rvert < 80\,{\rm MeV}/c^2$
D_s^-	$\chi^2_{\rm IP} < 10$, $\chi^2_{\rm VS} > 50$, $\tau > 0.0002\,{\rm ns}$ ${\rm DIRA}_{\rm PV} > 0.9999$, $\chi^2_{\rm vertex}/{\rm ndf} < 10$, $\lvert m - 1968\,{\rm MeV}/c^2\rvert < 70\,{\rm MeV}/c^2$

Table 18: Description of `Hlt2PIDDs2MuMuPiPosTaggedTurboCalib` for TCK `0xDEADBEEF`: the draft 2016 configuration. This combines $\mathrm{D}_\mathrm{s}^+ \to \mu^+\mu^-\pi^+$.

μ^-	$\chi^2_{\mathrm{IP}} > 9$, $p_\mathrm{T} > 0\,\mathrm{MeV}/c$, $p > 3\,\mathrm{MeV}/c$, charge < 0 $\chi^2_{\mathrm{track}}/\mathrm{ndf} < 4$, `Hlt1.*Decision TIS` `L0(Muon|DiMuon)Decision TIS`, long track
π^+	$\chi^2_{\mathrm{IP}} > 9$, $p_\mathrm{T} > 200\,\mathrm{MeV}/c$, $p > 1000\,\mathrm{MeV}/c$, $\chi^2_{\mathrm{track}}/\mathrm{ndf} < 3$
μ^+	IsMuon, $\chi^2_{\mathrm{IP}} > 25$, $p_\mathrm{T} > 500\,\mathrm{MeV}/c$, $p > 3000\,\mathrm{MeV}/c$ GhostProb < 0.2, charge > 0, $\chi^2_{\mathrm{track}}/\mathrm{ndf} < 4$, HasMuon long track
$\mu^+\mu^-\pi^+$	$p_\mathrm{T}(\mu^+) + p_\mathrm{T}(\mu^-) + p_\mathrm{T}(\pi^+) > 2000\,\mathrm{MeV}/c$ NumChildren($\chi^2_{\mathrm{IP}} > 20$) ≥ 2 NumChildren($\chi^2_{\mathrm{IP}} > 40$) ≥ 1 NumChildren($p_\mathrm{T} > 200\,\mathrm{MeV}/c$) ≥ 2 NumChildren($p_\mathrm{T} > 400\,\mathrm{MeV}/c$) ≥ 1, $\lvert m - 1968\,\mathrm{MeV}/c^2\rvert < 80\,\mathrm{MeV}/c^2$
D_s^+	$\chi^2_{\mathrm{IP}} < 10$, $\chi^2_{\mathrm{VS}} > 50$, $\tau > 0.0002\,\mathrm{ns}$ $\mathrm{DIRA}_{\mathrm{PV}} > 0.9999$, $\chi^2_{\mathrm{vertex}}/\mathrm{ndf} < 10$, $\lvert m - 1968\,\mathrm{MeV}/c^2\rvert < 70\,\mathrm{MeV}/c^2$

Table 19: Description of `Hlt2PIDKs2PiPiLLTurboCalib` for TCKs `0x00FB0051`, `0x0106XXXX`, `0x010700A1`, `0x010800A2` and `0x011400A8`: the 2015, 25 ns configuration. This combines $\mathrm{K}^0_\mathrm{S} \to \pi^+\pi^-$.

π^+	$\chi^2_{\mathrm{IP}} > 36, \;\; \chi^2_{\mathrm{track}}/\mathrm{ndf} < 3$
$\pi^+\pi^-$	$\lvert m - m_{\mathrm{K}^0_\mathrm{S}}\rvert < 50\,\mathrm{MeV}/c^2$
K^0_S	$\chi^2_{\mathrm{VS}} > 25, \;\; \tau > 2.0\,\mathrm{ps}, \;\; \chi^2_{\mathrm{vertex}}/\mathrm{ndf} < 30, \;\; z_{\mathrm{vertex}} < 2200$ $\lvert\chi^2_{\mathrm{vertex}} - 8\rvert < 8, \;\; \lvert m - m_{\mathrm{K}^0_\mathrm{S}}\rvert < 30\,\mathrm{MeV}/c^2$ $\lvert m(\pi^+ \to \pi^+, \pi^- \to \overline{\mathrm{p}}) - m_{\Lambda^0}\rvert > 9\,\mathrm{MeV}/c^2$ $\lvert m(\pi^+ \to \mathrm{p}, \pi^- \to \pi^-) - m_{\Lambda^0}\rvert > 9\,\mathrm{MeV}/c^2$

Table 20: Description of `Hlt2PIDKs2PiPiLLTurboCalib` for TCK `0xDEADBEEF`: the draft 2016 configuration. This combines $\mathrm{K}^0_\mathrm{S} \to \pi^+\pi^-$.

π^+	$\chi^2_{\mathrm{IP}} > 36, \;\; \chi^2_{\mathrm{track}}/\mathrm{ndf} < 3$
$\pi^+\pi^-$	$\lvert m - m_{\mathrm{K}^0_\mathrm{S}}\rvert < 50\,\mathrm{MeV}/c^2$
K^0_S	$\chi^2_{\mathrm{IP}} < 150, \;\; \chi^2_{\mathrm{VS}} > 25, \;\; \tau > 2.0\,\mathrm{ps}, \;\; \chi^2_{\mathrm{vertex}}/\mathrm{ndf} < 30$ $z_{\mathrm{vertex}} < 2200, \;\; \lvert\chi^2_{\mathrm{vertex}} - 8\rvert < 8, \;\; \lvert m - m_{\mathrm{K}^0_\mathrm{S}}\rvert < 30\,\mathrm{MeV}/c^2$ $\lvert m(\pi^+ \to \pi^+, \pi^- \to \overline{\mathrm{p}}) - m_{\Lambda^0}\rvert > 9\,\mathrm{MeV}/c^2$ $\lvert m(\pi^+ \to \mathrm{p}, \pi^- \to \pi^-) - m_{\Lambda^0}\rvert > 9\,\mathrm{MeV}/c^2$

Table 21: Description of `Hlt2PIDLambda2PPiLLTurboCalib` for TCKs `0x00F8014E` and `0x00F9014E`: the EM configuration. This combines $\Lambda^0 \to \mathrm{p}\pi^-$.

p	$\chi^2_{\mathrm{IP}} > 36, \;\; p_{\mathrm{T}} > 0\,\mathrm{MeV}/c, \;\; p > 2000\,\mathrm{MeV}/c, \;\; \chi^2_{\mathrm{track}}/\mathrm{ndf} < 4$
π^+	$\chi^2_{\mathrm{IP}} > 36, \;\; \chi^2_{\mathrm{track}}/\mathrm{ndf} < 4$
$\mathrm{p}\pi^-$	$\lvert m - m_{\Lambda^0}\rvert < 50\,\mathrm{MeV}/c^2$
Λ^0	$\tau > 2.0\,\mathrm{ps}, \;\; \chi^2_{\mathrm{vertex}}/\mathrm{ndf} < 30, \;\; \lvert m - m_{\Lambda^0}\rvert < 20\,\mathrm{MeV}/c^2$ $\lvert m(\mathrm{p} \to \pi^+, \pi^- \to \pi^-) - m_{\mathrm{K}^0_\mathrm{S}}\rvert > 20\,\mathrm{MeV}/c^2$

Table 22: Description of `Hlt2PIDLambda2PPiLLTurboCalib` for TCKs `0x00FB0051`, `0x0106XXXX`, `0x010700A1`, `0x010800A2`, `0x011400A8` and `0xDEADBEEF`: the 2015, 25 ns configuration. This combines $\Lambda^0 \to \mathrm{p}\pi^-$.

p	$\chi^2_{\mathrm{IP}} > 36,\ \ p_{\mathrm{T}} > 0\,\mathrm{MeV}/c,\ \ p > 2000\,\mathrm{MeV}/c,\ \ \chi^2_{\mathrm{track}}/\mathrm{ndf} < 4$
π^+	$\chi^2_{\mathrm{IP}} > 36,\ \ \chi^2_{\mathrm{track}}/\mathrm{ndf} < 4$
$\mathrm{p}\pi^-$	$\lvert m - m_{\Lambda^0}\rvert < 50\,\mathrm{MeV}/c^2$
Λ^0	$\chi^2_{\mathrm{IP}} < 50,\ \ \tau > 2.0\,\mathrm{ps},\ \ \chi^2_{\mathrm{vertex}}/\mathrm{ndf} < 30$ $\lvert m - m_{\Lambda^0}\rvert < 20\,\mathrm{MeV}/c^2,\ \ \lvert m(\mathrm{p}\to\pi^+,\pi^-\to\pi^-) - m_{\mathrm{K}^0_{\mathrm{S}}}\rvert > 20\,\mathrm{MeV}/c^2$

Table 23: Description of `Hlt2PIDLambda2PPiLLhighPTTurboCalib` for TCKs `0x00F8014E` and `0x00F9014E`: the EM configuration. This combines $\Lambda^0 \to \mathrm{p}\pi^-$.

p	$\chi^2_{\mathrm{IP}} > 36,\ \ p_{\mathrm{T}} > 3000\,\mathrm{MeV}/c,\ \ p > 2000\,\mathrm{MeV}/c,\ \ \chi^2_{\mathrm{track}}/\mathrm{ndf} < 4$
π^+	$\chi^2_{\mathrm{IP}} > 36,\ \ \chi^2_{\mathrm{track}}/\mathrm{ndf} < 4$
$\mathrm{p}\pi^-$	$\lvert m - m_{\Lambda^0}\rvert < 50\,\mathrm{MeV}/c^2$
Λ^0	$\tau > 2.0\,\mathrm{ps},\ \ \chi^2_{\mathrm{vertex}}/\mathrm{ndf} < 30,\ \ \lvert m - m_{\Lambda^0}\rvert < 20\,\mathrm{MeV}/c^2$ $\lvert m(\mathrm{p}\to\pi^+,\pi^-\to\pi^-) - m_{\mathrm{K}^0_{\mathrm{S}}}\rvert > 20\,\mathrm{MeV}/c^2$

Table 24: Description of `Hlt2PIDLambda2PPiLLhighPTTurboCalib` for TCKs `0x00FB0051`, `0x0106XXXX`, `0x010700A1`, `0x010800A2`, `0x011400A8` and `0xDEADBEEF`: the 2015, 25 ns configuration. This combines $\Lambda^0 \to \mathrm{p}\pi^-$.

p	$\chi^2_{\mathrm{IP}} > 36,\ \ p_{\mathrm{T}} > 3000\,\mathrm{MeV}/c,\ \ p > 2000\,\mathrm{MeV}/c,\ \ \chi^2_{\mathrm{track}}/\mathrm{ndf} < 4$
π^+	$\chi^2_{\mathrm{IP}} > 36,\ \ \chi^2_{\mathrm{track}}/\mathrm{ndf} < 4$
$\mathrm{p}\pi^-$	$\lvert m - m_{\Lambda^0}\rvert < 50\,\mathrm{MeV}/c^2$
Λ^0	$\chi^2_{\mathrm{IP}} < 50,\ \ \tau > 2.0\,\mathrm{ps},\ \ \chi^2_{\mathrm{vertex}}/\mathrm{ndf} < 30$ $\lvert m - m_{\Lambda^0}\rvert < 20\,\mathrm{MeV}/c^2,\ \ \lvert m(\mathrm{p}\to\pi^+,\pi^-\to\pi^-) - m_{\mathrm{K}^0_{\mathrm{S}}}\rvert > 20\,\mathrm{MeV}/c^2$

Table 25: Description of `Hlt2PIDLambda2PPiLLisMuonTurboCalib` for TCKs `0x00F8014E` and `0x00F9014E`: the EM configuration. This combines $\Lambda^0 \to \mathrm{p}\pi^-$.

p	IsMuonLoose, $\chi^2_{\mathrm{IP}} > 36$, $p_{\mathrm{T}} > 0\,\mathrm{MeV}/c$, $p > 2000\,\mathrm{MeV}/c$ $\chi^2_{\mathrm{track}}/\mathrm{ndf} < 4$
π^+	$\chi^2_{\mathrm{IP}} > 36$, $\chi^2_{\mathrm{track}}/\mathrm{ndf} < 4$
$\mathrm{p}\pi^-$	$\lvert m - m_{\Lambda^0}\rvert < 50\,\mathrm{MeV}/c^2$
Λ^0	$\tau > 2.0\,\mathrm{ps}$, $\chi^2_{\mathrm{vertex}}/\mathrm{ndf} < 30$, $\lvert m - m_{\Lambda^0}\rvert < 20\,\mathrm{MeV}/c^2$ $\lvert m(\mathrm{p}\to\pi^+,\pi^-\to\pi^-) - m_{\mathrm{K}^0_{\mathrm{S}}}\rvert > 20\,\mathrm{MeV}/c^2$

Table 26: Description of `Hlt2PIDLambda2PPiLLisMuonTurboCalib` for TCKs `0x00FB0051`, `0x0106XXXX`, `0x010700A1`, `0x010800A2`, `0x011400A8` and `0xDEADBEEF`: the 2015, 25 ns configuration. This combines $\Lambda^0 \to \mathrm{p}\pi^-$.

p	IsMuonLoose, $\chi^2_{\mathrm{IP}} > 36$, $p_{\mathrm{T}} > 0\,\mathrm{MeV}/c$, $p > 2000\,\mathrm{MeV}/c$ $\chi^2_{\mathrm{track}}/\mathrm{ndf} < 4$
π^+	$\chi^2_{\mathrm{IP}} > 36$, $\chi^2_{\mathrm{track}}/\mathrm{ndf} < 4$
$\mathrm{p}\pi^-$	$\lvert m - m_{\Lambda^0}\rvert < 50\,\mathrm{MeV}/c^2$
Λ^0	$\chi^2_{\mathrm{IP}} < 50$, $\tau > 2.0\,\mathrm{ps}$, $\chi^2_{\mathrm{vertex}}/\mathrm{ndf} < 30$ $\lvert m - m_{\Lambda^0}\rvert < 20\,\mathrm{MeV}/c^2$, $\lvert m(\mathrm{p}\to\pi^+,\pi^-\to\pi^-) - m_{\mathrm{K}^0_{\mathrm{S}}}\rvert > 20\,\mathrm{MeV}/c^2$

Table 27: Description of `Hlt2PIDLambda2PPiLLveryhighPTTurboCalib` for TCKs `0x00FB0051`, `0x0106XXXX`, `0x010700A1`, `0x010800A2`, `0x011400A8` and `0xDEADBEEF`: the 2015, 25 ns configuration. This combines $\Lambda^0 \to \mathrm{p}\pi^-$.

p	$\chi^2_{\mathrm{IP}} > 36$, $p_{\mathrm{T}} > 6000\,\mathrm{MeV}/c$, $p > 2000\,\mathrm{MeV}/c$, $\chi^2_{\mathrm{track}}/\mathrm{ndf} < 4$
π^+	$\chi^2_{\mathrm{IP}} > 36$, $\chi^2_{\mathrm{track}}/\mathrm{ndf} < 4$
$\mathrm{p}\pi^-$	$\lvert m - m_{\Lambda^0}\rvert < 50\,\mathrm{MeV}/c^2$
Λ^0	$\chi^2_{\mathrm{IP}} < 50$, $\tau > 2.0\,\mathrm{ps}$, $\chi^2_{\mathrm{vertex}}/\mathrm{ndf} < 30$ $\lvert m - m_{\Lambda^0}\rvert < 20\,\mathrm{MeV}/c^2$, $\lvert m(\mathrm{p}\to\pi^+,\pi^-\to\pi^-) - m_{\mathrm{K}^0_{\mathrm{S}}}\rvert > 20\,\mathrm{MeV}/c^2$

Table 28: Description of `Hlt2PIDLambda2PPiLLveryhighPTTurboCalib` for TCKs `0x00F8014E` and `0x00F9014E`: the EM configuration. This combines $\Lambda^0 \to \mathrm{p}\pi^-$.

p	$\chi^2_{\mathrm{IP}} > 36$, $p_{\mathrm{T}} > 6000\,\mathrm{MeV}/c$, $p > 2000\,\mathrm{MeV}/c$, $\chi^2_{\mathrm{track}}/\mathrm{ndf} < 4$
π^+	$\chi^2_{\mathrm{IP}} > 36$, $\chi^2_{\mathrm{track}}/\mathrm{ndf} < 4$
$\mathrm{p}\pi^-$	$\lvert m - m_{\Lambda^0}\rvert < 50\,\mathrm{MeV}/c^2$
Λ^0	$\tau > 2.0\,\mathrm{ps}$, $\chi^2_{\mathrm{vertex}}/\mathrm{ndf} < 30$, $\lvert m - m_{\Lambda^0}\rvert < 20\,\mathrm{MeV}/c^2$ $\lvert m(\mathrm{p}\to\pi^+, \pi^-\to\pi^-) - m_{\mathrm{K}^0_{\mathrm{S}}}\rvert > 20\,\mathrm{MeV}/c^2$

Table 29: Description of `Hlt2PIDLc2KPPiTurboCalib` for TCK `0xDEADBEEF`: the draft 2016 configuration. This combines $\Lambda_c^+ \to K^-p\pi^+$.

K^+	$\chi^2_{IP} > 9$, $DLL_{K\pi} > 5$, $p_T > 400\,MeV/c$, $p > 1000\,MeV/c$ GhostProb < 1, $\chi^2_{track}/ndf < 3$, HasRich
p	$\chi^2_{IP} > 6$, $p_T > 1000\,MeV/c$, $p > 1000\,MeV/c$, GhostProb < 1 $\chi^2_{track}/ndf < 3$
π^+	$\chi^2_{IP} > 9$, $DLL_{K\pi} < -5$, $p_T > 400\,MeV/c$, $p > 1000\,MeV/c$ GhostProb < 1, $\chi^2_{track}/ndf < 3$, HasRich
$K^-p\pi^+$	$p_T(K^-) + p_T(p) + p_T(\pi^+) > 2000\,MeV/c$ NumChildren$(\chi^2_{IP} > 12) \geq 2$ NumChildren$(\chi^2_{IP} > 16) \geq 1$ NumChildren$(p_T > 400\,MeV/c) \geq 1$ NumChildren$(p_T > 400\,MeV/c) \geq 2$, $\lvert m - 2286.5\,MeV/c^2\rvert < 85\,MeV/c^2$
Λ_c^+	$\chi^2_{IP} < 10$, $\chi^2_{VS} > 50$, $\tau > 0.00015\,ns$ $DIRA_{PV} > 0.99995$, $\chi^2_{vertex}/ndf < 10$ $m(K^- \to K^-, p \to \pi^+, \pi^+ \to \pi^+) > 1735\,MeV/c^2$ $\lvert m - 2286.5\,MeV/c^2\rvert < 75\,MeV/c^2$ $\lvert m(K^- \to K^-, p \to K^+, \pi^+ \to \pi^+) - 1968\,MeV/c^2\rvert > 20\,MeV/c^2$ $\lvert m(K^- \to K^-, p \to \pi^+, \pi^+ \to \pi^+) - 1870\,MeV/c^2\rvert > 20\,MeV/c^2$ `Hlt1(Two)?TrackMVADecision TOS`

Table 30: Description of `Hlt2PIDB2KJPsiEEPosTaggedTurboCalib` for TCKs `0x00FB0051`, `0x0106XXXX`, `0x010700A1`, `0x010800A2`, `0x011400A8` and `0xDEADBEEF`: the 2015, 25 ns configuration. This combines $B^+ \to J/\psi K^+$, and takes J/ψ input from `Hlt2/Hlt2PIDJPsiEEPosTaggedCombiner` (Tables 50, 51).

K^+	$\chi^2_{IP} > 9$, $DLL_{K\pi} > 5$, $p_T > 1000\,MeV/c$, $p > 3000\,MeV/c$ $\chi^2_{track}/ndf < 3$
$J/\psi K^+$	$p_T(J/\psi) + p_T(K^+) > 2000\,MeV/c$, $\lvert m - 5279\,MeV/c^2\rvert < 1110\,MeV/c^2$
B^+	$\chi^2_{IP} < 100$, $\chi^2_{VS} > 15$, $DIRA_{PV} > 0.9999$ $\chi^2_{vertex} < 25$, $\lvert m - 5279\,MeV/c^2\rvert < 1000\,MeV/c^2$

Table 31: Description of `Hlt2PIDB2KJPsiEESSTaggedTurboCalib` for TCKs `0x00F8014E` and `0x00F9014E`: the EM configuration. This combines $B^+ \to J/\psi K^+$, and takes J/ψ input from `Hlt2/Hlt2PIDJPsiEEPosTaggedCombiner` (Table 49).

K^+	$\chi^2_{IP} > 9$, $DLL_{K\pi} > 5$, $p_T > 1000\,\text{MeV}/c$, $p > 3000\,\text{MeV}/c$ $\chi^2_{track}/\text{ndf} < 3$
$J/\psi K^+$	$p_T(J/\psi) + p_T(K^+) > 2000\,\text{MeV}/c$, $\lvert m - 5279\,\text{MeV}/c^2\rvert < 1110\,\text{MeV}/c^2$
B^+	$\chi^2_{IP} < 100$, $\chi^2_{VS} > 50$, $\chi^2_{vertex} < 25$ $\lvert m - 5279\,\text{MeV}/c^2\rvert < 1000\,\text{MeV}/c^2$

Table 32: Description of `Hlt2PIDB2KJPsiMuMuPosTaggedTurboCalib` for TCKs `0x00FB0051`, `0x0106XXXX`, `0x010700A1`, `0x010800A2`, `0x011400A8` and `0xDEADBEEF`: the 2015, 25 ns configuration. This combines $B^+ \to J/\psi K^+$, and takes J/ψ input from `Hlt2/Hlt2PIDJPsiMuMuPosTaggedCombiner` (Tables 52, 53).

K^+	$\chi^2_{IP} > 9$, $DLL_{K\pi} > 5$, $p_T > 300\,\text{MeV}/c$, $p > 3000\,\text{MeV}/c$ $\chi^2_{track}/\text{ndf} < 3$
$J/\psi K^+$	$p_T(J/\psi) + p_T(K^+) > 2000\,\text{MeV}/c$, $\lvert m - 5279\,\text{MeV}/c^2\rvert < 520\,\text{MeV}/c^2$
B^+	$\chi^2_{IP} < 25$, $\chi^2_{VS} > 15$, $DIRA_{PV} > 0.9999$ $\chi^2_{vertex} < 25$, $\lvert m - 5279\,\text{MeV}/c^2\rvert < 500\,\text{MeV}/c^2$

Table 33: Description of `Hlt2PIDB2KJPsiPPPosTaggedTurboCalib` for TCKs `0x00FB0051`, `0x0106XXXX`, `0x010700A1`, `0x010800A2` and `0x011400A8`: the 2015, 25 ns configuration. This combines $B^+ \to J/\psi K^+$, and takes J/ψ input from `Hlt2/Hlt2PIDJPsiPPPosTaggedCombiner` (Table 54).

K^+	$\chi^2_{IP} > 9$, $DLL_{K\pi} > 5$, $p_T > 300\,\text{MeV}/c$, $p > 3000\,\text{MeV}/c$ $\chi^2_{track}/\text{ndf} < 3$
$J/\psi K^+$	$p_T(J/\psi) + p_T(K^+) > 2000\,\text{MeV}/c$, $\lvert m - 5279\,\text{MeV}/c^2\rvert < 520\,\text{MeV}/c^2$
B^+	$\chi^2_{IP} < 25$, $\chi^2_{VS} > 15$, $DIRA_{PV} > 0.9999$ $\chi^2_{vertex} < 25$, $\lvert m - 5279\,\text{MeV}/c^2\rvert < 500\,\text{MeV}/c^2$

Table 34: Description of `Hlt2PIDD02KPiPiPiTagTurboCalib` for TCKs `0x00FB0051`, `0x0106XXXX`, `0x010700A1`, `0x010800A2` and `0x011400A8`: the 2015, 25 ns configuration. This combines $D^{*+} \to D^0\pi^+$, and takes D^0 input from `Hlt2/Hlt2CharmHadPIDD02KPiPiPiMassFilter` (Table 47).

π^+	$p_T > 100\,\text{MeV}/c,\ \ p > 1000\,\text{MeV}/c,\ \ \chi^2_{\text{track}}/\text{ndf} < 3$
$D^0\pi^+$	$\lvert m(D^0) - m(D^{*+}) + 95\,\text{MeV}/c\rvert < 95\,\text{MeV}/c$
D^{*+}	$\chi^2_{\text{vertex}}/\text{ndf} < 15,\ \ \lvert m(D^0) - m(D^{*+}) + 85\,\text{MeV}/c\rvert < 85\,\text{MeV}/c$

Table 35: Description of `Hlt2PIDD02KPiTagTurboCalib` for TCKs `0x00F8014E` and `0x00F9014E`: the EM configuration. This combines $D^{*+} \to D^0\pi^+$, and takes D^0 input from `Hlt2/Hlt2CharmHadPIDD02KPiMassFilter` (Table 46).

π^+	$p_T > 100\,\text{MeV}/c,\ \ p > 1000\,\text{MeV}/c,\ \ \chi^2_{\text{track}}/\text{ndf} < 3$
$D^0\pi^+$	$\lvert m(D^0) - m(D^{*+}) + 82.5\,\text{MeV}/c\rvert < 82.5\,\text{MeV}/c$
D^{*+}	$\chi^2_{\text{vertex}}/\text{ndf} < 15,\ \ \lvert m(D^0) - m(D^{*+}) + 77.5\,\text{MeV}/c\rvert < 77.5\,\text{MeV}/c$

Table 36: Description of `Hlt2PIDD02KPiTagTurboCalib` for TCKs `0x00FB0051`, `0x0106XXXX`, `0x010700A1`, `0x010800A2`, `0x011400A8` and `0xDEADBEEF`: the 2015, 25 ns configuration. This combines $D^{*+} \to D^0\pi^+$, and takes D^0 input from `Hlt2/Hlt2PIDD02KPiPromptIPChi2FilterFilter` (Table 48).

π^+	$p_T > 100\,\text{MeV}/c,\ \ p > 1000\,\text{MeV}/c,\ \ \chi^2_{\text{track}}/\text{ndf} < 3$
$D^0\pi^+$	$\lvert m(D^0) - m(D^{*+}) + 82.5\,\text{MeV}/c\rvert < 82.5\,\text{MeV}/c$
D^{*+}	$\chi^2_{\text{vertex}}/\text{ndf} < 15,\ \ \lvert m(D^0) - m(D^{*+}) + 77.5\,\text{MeV}/c\rvert < 77.5\,\text{MeV}/c$

Table 37: Description of `Hlt2PIDDs2PiPhiKKPosTaggedTurboCalib` for TCKs `0x00FB0051`, `0x0106XXXX`, `0x010700A1`, `0x010800A2` and `0x011400A8`: the 2015, 25 ns configuration. This combines $\mathrm{D}_\mathrm{s}^+ \to \phi\pi^+$, and takes ϕ input from `Hlt2/Hlt2PIDPhiKKPosTaggedCombiner` (Table 58).

π^+	$\chi^2_{\mathrm{IP}} > 9$, $\mathrm{DLL}_{\mathrm{K}\pi} < -5$, $p_\mathrm{T} > 300\,\mathrm{MeV}/c$, $p > 3000\,\mathrm{MeV}/c$ $\chi^2_{\mathrm{track}}/\mathrm{ndf} < 3$
$\phi\pi^+$	$p_\mathrm{T}(\phi) + p_\mathrm{T}(\pi^+) > 1000\,\mathrm{MeV}/c$, $\lvert m - 1968\,\mathrm{MeV}/c^2\rvert < 80\,\mathrm{MeV}/c^2$
D_s^+	$\chi^2_{\mathrm{IP}} < 25$, $\chi^2_{\mathrm{VS}} > 50$, $\mathrm{DIRA}_{\mathrm{PV}} > 0.9999$ $\chi^2_{\mathrm{vertex}} < 25$, $\lvert m - 1968\,\mathrm{MeV}/c^2\rvert < 70\,\mathrm{MeV}/c^2$

Table 38: Description of `Hlt2PIDDs2PiPhiKKUnbiasedTurboCalib` for TCKs `0x00FB0051`, `0x0106XXXX`, `0x010700A1`, `0x010800A2` and `0x011400A8`: the 2015, 25 ns configuration. This combines $\mathrm{D}_\mathrm{s}^+ \to \phi\pi^+$, and takes ϕ input from `Hlt2/Hlt2PIDPhiKKUnbiasedCombiner` (Table 59).

π^+	$\chi^2_{\mathrm{IP}} > 9$, $\mathrm{DLL}_{\mathrm{K}\pi} < -5$, $p_\mathrm{T} > 300\,\mathrm{MeV}/c$, $p > 3000\,\mathrm{MeV}/c$ $\chi^2_{\mathrm{track}}/\mathrm{ndf} < 3$
$\phi\pi^+$	$p_\mathrm{T}(\phi) + p_\mathrm{T}(\pi^+) > 1000\,\mathrm{MeV}/c$, $\lvert m - 1968\,\mathrm{MeV}/c^2\rvert < 80\,\mathrm{MeV}/c^2$
D_s^+	$\chi^2_{\mathrm{IP}} < 25$, $\chi^2_{\mathrm{VS}} > 50$, $\mathrm{DIRA}_{\mathrm{PV}} > 0.9999$ $\chi^2_{\mathrm{vertex}} < 25$, $\lvert m - 1968\,\mathrm{MeV}/c^2\rvert < 70\,\mathrm{MeV}/c^2$

Table 39: Description of `Hlt2PIDDs2PiPhiMuMuPosTaggedTurboCalib` for TCKs `0x00FB0051`, `0x0106XXXX`, `0x010700A1`, `0x010800A2` and `0x011400A8`: the 2015, 25 ns configuration. This combines $D_s^+ \to \phi\pi^+$, and takes ϕ input from `Hlt2/Hlt2PIDPhiMuMuPosTaggedCombiner` (Table 60).

π^+	$\chi^2_{\rm IP} > 9$, $\mathrm{DLL}_{K\pi} < -5$, $p_T > 300\,\mathrm{MeV}/c$, $p > 3000\,\mathrm{MeV}/c$ $\chi^2_{\rm track}/\mathrm{ndf} < 3$
$\phi\pi^+$	$p_T(\phi) + p_T(\pi^+) > 1000\,\mathrm{MeV}/c$, $\lvert m - 1968\,\mathrm{MeV}/c^2\rvert < 80\,\mathrm{MeV}/c^2$
D_s^+	$\chi^2_{\rm IP} < 20$, $\chi^2_{\rm VS} > 50$, $\mathrm{DIRA}_{\rm PV} > 0.9999$ $\chi^2_{\rm vertex} < 25$, $\lvert m - 1968\,\mathrm{MeV}/c^2\rvert < 70\,\mathrm{MeV}/c^2$

Table 40: Description of `Hlt2PIDLb2LcMuNuTurboCalib` for TCKs `0x00F8014E` and `0x00F9014E`: the EM configuration. This combines $\Lambda_b^0 \to \Lambda_c^+\mu^-$, and takes Λ_c^+ input from `Hlt2/Hlt2PIDLc2KPPiVetoFilter` (Table 56).

μ^+	IsMuon, $\chi^2_{\rm IP} > 16$, $\mathrm{DLL}_{\mu\pi} > 0$, $p_T > 500\,\mathrm{MeV}/c$, $p > 3000\,\mathrm{MeV}/c$ $\chi^2_{\rm track}/\mathrm{ndf} < 5$, HasMuon
$\Lambda_c^+\mu^-$	$p_T(\Lambda_c^+) + p_T(\mu^-) > 3000\,\mathrm{MeV}/c$, $\lvert m - 3010\,\mathrm{MeV}/c^2\rvert < 3010\,\mathrm{MeV}/c^2$
Λ_b^0	$\chi^2_{\rm IP} < 200$, $\chi^2_{\rm VS} > 100$, $\chi^2_{\rm vertex} < 25$ $\lvert m_{\rm corr.} - 5270\,\mathrm{MeV}/c^2\rvert < 750\,\mathrm{MeV}/c^2$

Table 41: Description of `Hlt2PIDLb2LcMuNuTurboCalib` for TCKs `0x00FB0051`, `0x0106XXXX`, `0x010700A1`, `0x010800A2`, `0x011400A8` and `0xDEADBEEF`: the 2015, 25 ns configuration. This combines $\Lambda_b^0 \to \Lambda_c^+\mu^-$, and takes Λ_c^+ input from `Hlt2/Hlt2PIDLc2KPPiVetoFilter` (Tables 56, 57).

μ^+	IsMuon, $\chi^2_{\rm IP} > 16$, $\mathrm{DLL}_{\mu\pi} > 0$, $p_T > 500\,\mathrm{MeV}/c$, $p > 3000\,\mathrm{MeV}/c$ $\chi^2_{\rm track}/\mathrm{ndf} < 5$, HasMuon
$\Lambda_c^+\mu^-$	$p_T(\Lambda_c^+) + p_T(\mu^-) > 3000\,\mathrm{MeV}/c$, $\lvert m - 3010\,\mathrm{MeV}/c^2\rvert < 3010\,\mathrm{MeV}/c^2$
Λ_b^0	$\chi^2_{\rm IP} < 200$, $\chi^2_{\rm VS} > 100$, $\mathrm{DIRA}_{\rm PV} > 0.99$ $\chi^2_{\rm vertex} < 25$, $\lvert m_{\rm corr.} - 5270\,\mathrm{MeV}/c^2\rvert < 750\,\mathrm{MeV}/c^2$

Table 42: Description of `Hlt2PIDLb2LcPiTurboCalib` for TCKs `0x00F8014E` and `0x00F9014E`: the EM configuration. This combines $\Lambda_b^0 \to \Lambda_c^+\pi^-$, and takes Λ_c^+ input from `Hlt2/Hlt2PIDLc2KPPiVetoFilter` (Table 56).

π^+	$\chi^2_{\rm IP} > 25$, $\mathrm{DLL}_{K\pi} < -5$, $p_T > 500\,\mathrm{MeV}/c$, $p > 3000\,\mathrm{MeV}/c$ $\chi^2_{\rm track}/\mathrm{ndf} < 3$
$\Lambda_c^+\pi^-$	$p_T(\Lambda_c^+) + p_T(\pi^-) > 3000\,\mathrm{MeV}/c$, $\lvert m - 5620\,\mathrm{MeV}/c^2\rvert < 350\,\mathrm{MeV}/c^2$
Λ_b^0	$\chi^2_{\rm IP} < 10$, $\chi^2_{\rm VS} > 100$, $\chi^2_{\rm vertex} < 25$ $\lvert m - 5620\,\mathrm{MeV}/c^2\rvert < 300\,\mathrm{MeV}/c^2$

Table 43: Description of `Hlt2PIDLb2LcPiTurboCalib` for TCKs `0x00FB0051`, `0x0106XXXX`, `0x010700A1`, `0x010800A2`, `0x011400A8` and `0xDEADBEEF`: the 2015, 25 ns configuration. This combines $\Lambda_b^0 \to \Lambda_c^+\pi^-$, and takes Λ_c^+ input from `Hlt2/Hlt2PIDLc2KPPiVetoFilter` (Tables 56, 57).

π^+	$\chi^2_{\rm IP} > 25$, $\mathrm{DLL}_{K\pi} < -5$, $p_T > 500\,\mathrm{MeV}/c$, $p > 3000\,\mathrm{MeV}/c$ $\chi^2_{\rm track}/\mathrm{ndf} < 3$
$\Lambda_c^+\pi^-$	$p_T(\Lambda_c^+) + p_T(\pi^-) > 3000\,\mathrm{MeV}/c$, $\lvert m - 5620\,\mathrm{MeV}/c^2\rvert < 350\,\mathrm{MeV}/c^2$
Λ_b^0	$\chi^2_{\rm IP} < 10$, $\chi^2_{\rm VS} > 100$, $\mathrm{DIRA}_{\rm PV} > 0.9999$ $\chi^2_{\rm vertex} < 25$, $\lvert m - 5620\,\mathrm{MeV}/c^2\rvert < 300\,\mathrm{MeV}/c^2$

Table 44: Description of `Hlt2PIDSc02LcPiTurboCalib` for TCKs `0x00FB0051`, `0x0106XXXX`, `0x010700A1`, `0x010800A2` and `0x011400A8`: the 2015, 25 ns configuration. This combines $\Sigma_c^0 \to \Lambda_c^+\pi^-$, and takes Λ_c^+ input from `Hlt2/Hlt2PIDLc2KPPiPromptPromptFilterTisTosTagger` (Table 55).

π^+	$p_T > 100\,\mathrm{MeV}/c$, $p > 1000\,\mathrm{MeV}/c$, $\chi^2_{\rm track}/\mathrm{ndf} < 3$
$\Lambda_c^+\pi^-$	$\lvert m(\Lambda_c^+) - m(\Sigma_c^0) + 212.5\,\mathrm{MeV}/c\rvert < 62.5\,\mathrm{MeV}/c$
Σ_c^0	$\chi^2_{\rm vertex}/\mathrm{ndf} < 50$, $\lvert m(\Lambda_c^+) - m(\Sigma_c^0) + 212.5\,\mathrm{MeV}/c\rvert < 57.5\,\mathrm{MeV}/c$

Table 45: Description of `Hlt2PIDScpp2LcPiTurboCalib` for TCKs `0x00FB0051`, `0x0106XXXX`, `0x010700A1`, `0x010800A2` and `0x011400A8`: the 2015, 25 ns configuration. This combines $\Sigma_c^{++} \to \Lambda_c^+\pi^+$, and takes Λ_c^+ input from `Hlt2/Hlt2PIDLc2KPPiPromptPromptFilterTisTosTagger` (Table 55).

π^+	$p_{\rm T} > 100\,{\rm MeV}/c$, $p > 1000\,{\rm MeV}/c$, $\chi^2_{\rm track}/{\rm ndf} < 3$
$\Lambda_c^+\pi^+$	$\lvert m(\Lambda_c^+) - m(\Sigma_c^{++}) + 212.5\,{\rm MeV}/c\rvert < 62.5\,{\rm MeV}/c$
Σ_c^{++}	$\chi^2_{\rm vertex}/{\rm ndf} < 50$, $\lvert m(\Lambda_c^+) - m(\Sigma_c^{++}) + 212.5\,{\rm MeV}/c\rvert < 57.5\,{\rm MeV}/c$

Table 46: Description of `Hlt2/Hlt2CharmHadPIDD02KPiMassFilter` for TCKs `0x00F8014E` and `0x00F9014E`: the EM configuration. This combines $D^0 \to K^-\pi^+$.

K^+, π^+	$\chi^2_{\rm IP} > 16$, $p_{\rm T} > 250\,{\rm MeV}/c$, $p > 2000\,{\rm MeV}/c$, $\chi^2_{\rm track}/{\rm ndf} < 3$
$K^-\pi^+$	$\max(K^- p_{\rm T}, \pi^+ p_{\rm T}) > 1000\,{\rm MeV}/c$, $DOCA(K^-, \pi^+) < 0.1\,{\rm mm}$, $p_{\rm T} > 1500\,{\rm MeV}/c$ $\lvert m - 1865\,{\rm MeV}/c^2\rvert < 85\,{\rm MeV}/c^2$
D^0	$\chi^2_{\rm VS} > 49$, ${\rm DIRA}_{\rm PV} > 0.9999$, $\chi^2_{\rm vertex}/{\rm ndf} < 10$ $\lvert m - 1865\,{\rm MeV}/c^2\rvert < 75\,{\rm MeV}/c^2$

Table 47: Description of `Hlt2/Hlt2CharmHadPIDD02KPiPiPiMassFilter` for TCKs `0x00FB0051`, `0x0106XXXX`, `0x010700A1`, `0x010800A2` and `0x011400A8`: the 2015, 25 ns configuration. This combines $D^0 \to K^-\pi^+\pi^+\pi^-$.

K^+, π^+	$\chi^2_{\rm IP} > 3$, $p_{\rm T} > 250\,{\rm MeV}/c$, $p > 1000\,{\rm MeV}/c$, $\chi^2_{\rm track}/{\rm ndf} < 3$
$K^-\pi^+$	$DOCA(K^-, \pi^+) < 100\,{\rm mm}$, $\chi^2_{\rm DOCA}(K^-, \pi^+) < 10$, $m < 1671\,{\rm MeV}/c^2$
$K^-\pi^+\pi^+$	$DOCA(K^-, \pi^+) < 100\,{\rm mm}$, $DOCA(\pi^+, \pi^+) < 100\,{\rm mm}$ $\chi^2_{\rm DOCA}(K^-, \pi^+) < 10$, $\chi^2_{\rm DOCA}(\pi^+, \pi^+) < 10$ $m < 1810.5\,{\rm MeV}/c^2$
$K^-\pi^+\pi^+\pi^-$	$DOCA(K^-, \pi^-) < 100\,{\rm mm}$, $DOCA(\pi^+, \pi^-) < 100\,{\rm mm}$ $DOCA(\pi^+, \pi^-) < 100\,{\rm mm}$, $\chi^2_{\rm DOCA}(K^-, \pi^-) < 10$ $\chi^2_{\rm DOCA}(\pi^+, \pi^-) < 10$, $\chi^2_{\rm DOCA}(\pi^+, \pi^-) < 10$ $p_{\rm T}(K^-) + p_{\rm T}(\pi^+) + p_{\rm T}(\pi^+) + p_{\rm T}(\pi^-) > 2500\,{\rm MeV}/c$ $p > 25000\,{\rm MeV}/c$, $\lvert m - 1865\,{\rm MeV}/c^2\rvert < 85\,{\rm MeV}/c^2$
D^0	$\chi^2_{\rm VS} > 25$, $p_{\rm T} > 2000\,{\rm MeV}/c$, $p > 30000\,{\rm MeV}/c$, $\tau > 0.0001\,{\rm ns}$ ${\rm DIRA}_{\rm PV} > 0.9999$, $\chi^2_{\rm vertex}/{\rm ndf} < 12$, $\lvert m - 1865\,{\rm MeV}/c^2\rvert < 75\,{\rm MeV}/c^2$ `Hlt1.*Track.*Decision TOS`

Table 48: Description of `Hlt2/Hlt2PIDD02KPiPromptIPChi2FilterFilter` for TCKs `0x00FB0051`, `0x0106XXXX`, `0x010700A1`, `0x010800A2`, `0x011400A8` and `0xDEADBEEF`: the 2015, 25 ns configuration. This combines $D^0 \to K^-\pi^+$.

K^+, π^+	$\chi^2_{\rm IP} > 16$, $p_{\rm T} > 250\,{\rm MeV}/c$, $p > 2000\,{\rm MeV}/c$, $\chi^2_{\rm track}/{\rm ndf} < 3$
$K^-\pi^+$	$\max(K^- p_{\rm T}, \pi^+ p_{\rm T}) > 1000\,{\rm MeV}/c$, $DOCA(K^-, \pi^+) < 0.1\,{\rm mm}$, $p_{\rm T} > 1500\,{\rm MeV}/c$ $\lvert m - 1865\,{\rm MeV}/c^2\rvert < 85\,{\rm MeV}/c^2$
D^0	$\chi^2_{\rm IP} < 20$, $\chi^2_{\rm VS} > 49$, ${\rm DIRA}_{\rm PV} > 0.9999$ $\chi^2_{\rm vertex}/{\rm ndf} < 10$, $\lvert m - 1865\,{\rm MeV}/c^2\rvert < 75\,{\rm MeV}/c^2$

Table 49: Description of `Hlt2/Hlt2PIDJPsiEEPosTaggedCombiner` for TCKs `0x00F8014E` and `0x00F9014E`: the EM configuration. This combines $J/\psi \to e^+e^-$.

e^-	$\chi^2_{IP} > 25$, $p_T > 500\,\text{MeV}/c$, $p > 3000\,\text{MeV}/c$, charge < 0 $\chi^2_{track}/\text{ndf} < 5$, long track
e^+	$\chi^2_{IP} > 9$, $\text{DLL}_{e\pi} > 5$, $p_T > 1500\,\text{MeV}/c$, $p > 6000\,\text{MeV}/c$ charge > 0, $\chi^2_{track}/\text{ndf} < 3$, HasCalo, long track
e^+e^-	$\chi^2_{DOCA}(e^+, e^-) < 18$, $\lvert m - 2896\,\text{MeV}/c^2\rvert < 710\,\text{MeV}/c^2$
J/ψ	$\lvert m - 2896\,\text{MeV}/c^2\rvert < 700\,\text{MeV}/c^2$

Table 50: Description of `Hlt2/Hlt2PIDJPsiEEPosTaggedCombiner` for TCKs `0x00FB0051`, `0x0106XXXX`, `0x010700A1`, `0x010800A2` and `0x011400A8`: the 2015, 25 ns configuration. This combines $J/\psi \to e^+e^-$.

e^-	$\chi^2_{IP} > 9$, $p_T > 500\,\text{MeV}/c$, $p > 3000\,\text{MeV}/c$, charge < 0 $\chi^2_{track}/\text{ndf} < 5$, `Hlt1.*Decision TIS`, long track `L0(Photon|Electron|Hadron|Muon|DiMuon)Decision TIS`
e^+	$\chi^2_{IP} > 25$, $\text{DLL}_{e\pi} > 5$, $p_T > 1500\,\text{MeV}/c$, $p > 6000\,\text{MeV}/c$ GhostProb < 1, charge > 0, $\chi^2_{track}/\text{ndf} < 5$, HasCalo long track
e^+e^-	$\chi^2_{DOCA}(e^+, e^-) < 18$, $\lvert m - 2896\,\text{MeV}/c^2\rvert < 710\,\text{MeV}/c^2$
J/ψ	$\lvert m - 2896\,\text{MeV}/c^2\rvert < 700\,\text{MeV}/c^2$

Table 51: Description of `Hlt2/Hlt2PIDJPsiEEPosTaggedCombiner` for TCK `0xDEADBEEF`: the draft 2016 configuration. This combines $J/\psi \to e^+e^-$.

e^-	$\chi^2_{IP} > 9$, $p_T > 500\,\text{MeV}/c$, $p > 3000\,\text{MeV}/c$, charge < 0 $\chi^2_{track}/\text{ndf} < 4$, `Hlt1.*Decision TIS`, long track `L0(Photon|Electron|Hadron|Muon|DiMuon)Decision TIS`
e^+	$\chi^2_{IP} > 25$, $\text{DLL}_{e\pi} > 5$, $p_T > 1500\,\text{MeV}/c$, $p > 6000\,\text{MeV}/c$ GhostProb < 1, charge > 0, $\chi^2_{track}/\text{ndf} < 4$, HasCalo long track
e^+e^-	$\chi^2_{DOCA}(e^+, e^-) < 18$, $\lvert m - 2896\,\text{MeV}/c^2\rvert < 710\,\text{MeV}/c^2$
J/ψ	$\lvert m - 2896\,\text{MeV}/c^2\rvert < 700\,\text{MeV}/c^2$

Table 52: Description of `Hlt2/Hlt2PIDJPsiMuMuPosTaggedCombiner` for TCKs `0x00FB0051`, `0x0106XXXX`, `0x010700A1`, `0x010800A2` and `0x011400A8`: the 2015, 25 ns configuration. This combines $J/\psi \to \mu^+\mu^-$.

μ^-	$\chi^2_{\rm IP} > 9$, $p_{\rm T} > 0\,{\rm MeV}/c$, $p > 3000\,{\rm MeV}/c$, charge < 0 $\chi^2_{\rm track}/{\rm ndf} < 5$, `L0(Muon|DiMuon)Decision TIS`, long track `Hlt1(TrackAllL0|TrackMuon|SingleMuon|DiMuon|TrackMVA|TwoTrackMVA).*Decision TIS`
μ^+	IsMuon, $\chi^2_{\rm IP} > 9$, $p_{\rm T} > 1200\,{\rm MeV}/c$, $p > 3000\,{\rm MeV}/c$ GhostProb < 0.2, charge > 0, $\chi^2_{\rm track}/{\rm ndf} < 3$, HasMuon long track
$\mu^+\mu^-$	$\chi^2_{\rm DOCA}(\mu^+, \mu^-) < 10$, $\lvert m - 3096\,{\rm MeV}/c^2\rvert < 210\,{\rm MeV}/c^2$
J/ψ	$\lvert m - 3096\,{\rm MeV}/c^2\rvert < 200\,{\rm MeV}/c^2$

Table 53: Description of `Hlt2/Hlt2PIDJPsiMuMuPosTaggedCombiner` for TCK `0xDEADBEEF`: the draft 2016 configuration. This combines $J/\psi \to \mu^+\mu^-$.

μ^-	$\chi^2_{\rm IP} > 20$, $p_{\rm T} > 0\,{\rm MeV}/c$, $p > 3000\,{\rm MeV}/c$, charge < 0 $\chi^2_{\rm track}/{\rm ndf} < 4$, `Hlt1.*Decision TIS` `L0(Muon|DiMuon)Decision TIS`, long track
μ^+	IsMuon, $\chi^2_{\rm IP} > 9$, $p_{\rm T} > 1200\,{\rm MeV}/c$, $p > 3000\,{\rm MeV}/c$ GhostProb < 0.2, charge > 0, $\chi^2_{\rm track}/{\rm ndf} < 4$, HasMuon long track
$\mu^+\mu^-$	$\chi^2_{\rm DOCA}(\mu^+, \mu^-) < 5$, $\lvert m - 3071\,{\rm MeV}/c^2\rvert < 185\,{\rm MeV}/c^2$
J/ψ	$\lvert m - 3071\,{\rm MeV}/c^2\rvert < 175\,{\rm MeV}/c^2$

Table 54: Description of `Hlt2/Hlt2PIDJPsiPPPosTaggedCombiner` for TCKs `0x00FB0051`, `0x0106XXXX`, `0x010700A1`, `0x010800A2` and `0x011400A8`: the 2015, 25 ns configuration. This combines $J/\psi \to p\overline{p}$.

p	$\chi^2_{IP} > 25$, $DLL_{p\pi} > 5$, $p_T > 1500\,MeV/c$, $p > 3000\,MeV/c$ GhostProb < 0.2, charge > 0, $\chi^2_{track}/ndf < 3$, HasRich long track
$\overline{p}$	$\chi^2_{IP} > 16$, $p_T > 800\,MeV/c$, $p > 3000\,MeV/c$, charge < 0 $\chi^2_{track}/ndf < 5$, long track
$p\overline{p}$	$\chi^2_{DOCA}(p, \overline{p}) < 10$, $\lvert m - 3096\,MeV/c^2\rvert < 220\,MeV/c^2$
J/ψ	$\lvert m - 3096\,MeV/c^2\rvert < 200\,MeV/c^2$

Table 55: Description of `Hlt2/Hlt2PIDLc2KPPiPromptPromptFilterTisTosTagger` for TCKs `0x00FB0051`, `0x0106XXXX`, `0x010700A1`, `0x010800A2` and `0x011400A8`: the 2015, 25 ns configuration. This combines $\Lambda_c^+ \to K^-p\pi^+$.

K^+	$\chi^2_{IP} > 9$, $DLL_{K\pi} > 5$, $p_T > 400\,MeV/c$, $p > 1000\,MeV/c$ GhostProb < 1000000000, $\chi^2_{track}/ndf < 3$, HasRich
p	$\chi^2_{IP} > 6$, $p_T > 1000\,MeV/c$, $p > 1000\,MeV/c$ GhostProb < 1000000000, $\chi^2_{track}/ndf < 3$
π^+	$\chi^2_{IP} > 9$, $DLL_{K\pi} < -5$, $p_T > 400\,MeV/c$, $p > 1000\,MeV/c$ GhostProb < 1000000000, $\chi^2_{track}/ndf < 3$, HasRich
$K^-p\pi^+$	$p_T(K^-) + p_T(p) + p_T(\pi^+) > 2000\,MeV/c$ NumChildren($\chi^2_{IP} > 12$) ≥ 2 NumChildren($\chi^2_{IP} > 16$) ≥ 1 NumChildren($p_T > 400\,MeV/c$) ≥ 1 NumChildren($p_T > 400\,MeV/c$) ≥ 2, $\lvert m - 2286.5\,MeV/c^2\rvert < 85\,MeV/c^2$
Λ_c^+	$\chi^2_{VS} > 50$, $\tau > 0.00015\,ns$, $DIRA_{PV} > 0.99995$ $\chi^2_{vertex}/ndf < 10$, $\lvert m - 2286.5\,MeV/c^2\rvert < 75\,MeV/c^2$ $\lvert m(K^-\pi^+) - 896\,MeV/c^2\rvert < 100\,MeV/c^2$ $\lvert m(K^- \to K^-, p \to K^+, \pi^+ \to \pi^+) - 1968\,MeV/c^2\rvert > 15\,MeV/c^2$ $\lvert m(K^- \to K^-, p \to \pi^+, \pi^+ \to \pi^+) - 1870\,MeV/c^2\rvert > 15\,MeV/c^2$ `Hlt1(Two)?TrackMVADecision TOS`

Table 56: Description of `Hlt2/Hlt2PIDLc2KPPiVetoFilter` for TCKs `0x00F8014E`, `0x00F9014E`, `0x00FB0051`, `0x0106XXXX`, `0x010700A1`, `0x010800A2` and `0x011400A8`: the EM configuration. This combines $\Lambda_c^+ \to K^- p \pi^+$.

K^+	$\chi^2_{IP} > 9$, $DLL_{K\pi} > 5$, $p_T > 400\,MeV/c$, $p > 1000\,MeV/c$ GhostProb < 1000000000, $\chi^2_{track}/ndf < 3$, HasRich
p	$\chi^2_{IP} > 6$, $p_T > 1000\,MeV/c$, $p > 1000\,MeV/c$ GhostProb < 1000000000, $\chi^2_{track}/ndf < 3$
π^+	$\chi^2_{IP} > 9$, $DLL_{K\pi} < -5$, $p_T > 400\,MeV/c$, $p > 1000\,MeV/c$ GhostProb < 1000000000, $\chi^2_{track}/ndf < 3$, HasRich
$K^- p \pi^+$	$p_T(K^-) + p_T(p) + p_T(\pi^+) > 2000\,MeV/c$ NumChildren$(\chi^2_{IP} > 12) \geq 2$ NumChildren$(\chi^2_{IP} > 16) \geq 1$ NumChildren$(p_T > 400\,MeV/c) \geq 1$ NumChildren$(p_T > 400\,MeV/c) \geq 2$, $\lvert m - 2286.5\,MeV/c^2\rvert < 85\,MeV/c^2$
Λ_c^+	$\chi^2_{VS} > 50$, $\tau > 0.0001\,ns$, $DIRA_{PV} > 0$ $\chi^2_{vertex}/ndf < 10$, $\lvert m - 2286.5\,MeV/c^2\rvert < 75\,MeV/c^2$ $\lvert m(K^-\pi^+) - 896\,MeV/c^2\rvert < 100\,MeV/c^2$ $\lvert m(K^- \to K^-, p \to K^+, \pi^+ \to \pi^+) - 1968\,MeV/c^2\rvert > 15\,MeV/c^2$ $\lvert m(K^- \to K^-, p \to \pi^+, \pi^+ \to \pi^+) - 1870\,MeV/c^2\rvert > 15\,MeV/c^2$

Table 57: Description of `Hlt2/Hlt2PIDLc2KPPiVetoFilter` for TCK `0xDEADBEEF`: the draft 2016 configuration. This combines $\Lambda_c^+ \to K^-p\pi^+$.

K^+	$\chi^2_{IP} > 9$, $DLL_{K\pi} > 5$, $p_T > 400\,MeV/c$, $p > 1000\,MeV/c$ GhostProb < 1, $\chi^2_{track}/ndf < 3$, HasRich
p	$\chi^2_{IP} > 6$, $p_T > 1000\,MeV/c$, $p > 1000\,MeV/c$, GhostProb < 1 $\chi^2_{track}/ndf < 3$
π^+	$\chi^2_{IP} > 9$, $DLL_{K\pi} < -5$, $p_T > 400\,MeV/c$, $p > 1000\,MeV/c$ GhostProb < 1, $\chi^2_{track}/ndf < 3$, HasRich
$K^-p\pi^+$	$p_T(K^-) + p_T(p) + p_T(\pi^+) > 2000\,MeV/c$ NumChildren($\chi^2_{IP} > 12$) ≥ 2 NumChildren($\chi^2_{IP} > 16$) ≥ 1 NumChildren($p_T > 400\,MeV/c$) ≥ 1 NumChildren($p_T > 400\,MeV/c$) ≥ 2, $\lvert m - 2286.5\,MeV/c^2\rvert < 85\,MeV/c^2$
Λ_c^+	$\chi^2_{VS} > 50$, $\tau > 0.0001\,ns$, $DIRA_{PV} > 0$ $\chi^2_{vertex}/ndf < 10$, $m(K^- \to K^-, p \to \pi^+, \pi^+ \to \pi^+) > 1735\,MeV/c^2$ $\lvert m - 2286.5\,MeV/c^2\rvert < 75\,MeV/c^2$ $\lvert m(K^- \to K^-, p \to K^+, \pi^+ \to \pi^+) - 1968\,MeV/c^2\rvert > 20\,MeV/c^2$ $\lvert m(K^- \to K^-, p \to \pi^+, \pi^+ \to \pi^+) - 1870\,MeV/c^2\rvert > 20\,MeV/c^2$

Table 58: Description of `Hlt2/Hlt2PIDPhiKKPosTaggedCombiner` for TCKs `0x00FB0051`, `0x0106XXXX`, `0x010700A1`, `0x010800A2` and `0x011400A8`: the 2015, 25 ns configuration. This combines $\phi \to K^+K^-$.

K^+	$\chi^2_{IP} > 16$, $DLL_{K\pi} > 0$, $p_T > 200\,MeV/c$, $p > 3000\,MeV/c$ GhostProb < 0.2, charge > 0, $\chi^2_{track}/ndf < 3$, HasRich long track
K^-	$\chi^2_{IP} > 9$, $p_T > 0\,MeV/c$, $p > 3000\,MeV/c$, charge < 0 $\chi^2_{track}/ndf < 5$, long track
K^+K^-	$\chi^2_{DOCA}(K^+, K^-) < 15$, $\lvert m - 1020\,MeV/c^2\rvert < 40\,MeV/c^2$
ϕ	$\lvert m - 1020\,MeV/c^2\rvert < 20\,MeV/c^2$

Table 59: Description of `Hlt2/Hlt2PIDPhiKKUnbiasedCombiner` for TCKs `0x00FB0051`, `0x0106XXXX`, `0x010700A1`, `0x010800A2` and `0x011400A8`: the 2015, 25 ns configuration. This combines $\phi \to K^+K^-$.

K^+	$\chi^2_{IP} > 16$, $p_T > 0\,\text{MeV}/c$
K^+K^-	$\chi^2_{DOCA}(K^+, K^-) < 15$, $p_T(K^+) + p_T(K^-) > 200\,\text{MeV}/c$ NumChildren($\chi^2_{IP} > 40$) ≥ 1 NumChildren($p_T > 200\,\text{MeV}/c$) ≥ 1, $\lvert m - m_\phi \rvert < 40\,\text{MeV}/c^2$
ϕ	$\lvert m - m_\phi \rvert < 20\,\text{MeV}/c^2$

Table 60: Description of `Hlt2/Hlt2PIDPhiMuMuPosTaggedCombiner` for TCKs `0x00FB0051`, `0x0106XXXX`, `0x010700A1`, `0x010800A2` and `0x011400A8`: the 2015, 25 ns configuration. This combines $\phi \to \mu^+\mu^-$.

μ^-	$\chi^2_{IP} > 9$, $p_T > 0\,\text{MeV}/c$, $p > 3000\,\text{MeV}/c$, charge < 0 $\chi^2_{track}/\text{ndf} < 5$, `L0(Muon|DiMuon)Decision TIS`, long track `Hlt1(TrackAllL0|TrackMuon|SingleMuon|DiMuon|TrackMVA|TwoTrackMVA).*Decision TIS`
μ^+	IsMuon, $\chi^2_{IP} > 25$, $p_T > 500\,\text{MeV}/c$, $p > 3000\,\text{MeV}/c$ GhostProb < 0.2, charge > 0, $\chi^2_{track}/\text{ndf} < 3$, HasMuon long track
$\mu^+\mu^-$	$\chi^2_{DOCA}(\mu^+, \mu^-) < 9$, $\lvert m - 1020\,\text{MeV}/c^2 \rvert < 40\,\text{MeV}/c^2$
ϕ	$\lvert m - 1020\,\text{MeV}/c^2 \rvert < 25\,\text{MeV}/c^2$